

Interdisciplinary Design — Design Report

Development of a Variable-
Friction Shoe Surface Mechanism

Michael Elliot King – 260345001

MECH 498 – Professor Rosaire Mongrain

Client & Supervisor: Professor Jeremy Cooperstock

DEPARTMENT OF MECHANICAL ENGINEERING
McGill University

December 6, 2013

Abstract

In order to treat and prevent accidents caused by balance-failure and friction-induced falls, a proper simulation environment is needed so users can be exposed to controlled slip conditions and trained to improve balance. This report covers the design of a mechanism that fits in the sole of a shoe and can dynamically actuate a brake that varies the coefficient of friction between the shoe and the walking surface. As it is vital to replicate a realistic sense of walking and slipping, the mechanism must be non-obtrusive and high-fidelity, and able to simulate a continuous range of surfaces, such as ice, wet grass, sand, or snow.

Contents

1	Introduction	1
Background	1	
Problem Definition	2	
Design Requirements	3	
2	Conceptual Design	4
Evaluation Criteria	4	
Cost	4	
Weight	5	
Complexity	5	
Robustness	5	
Size	5	
Concept Generation	5	
Concept Evaluation	6	
Final Concept	7	
3	Embodiment Design	10
Guidelines & Previous Research	10	
Calculations	12	
Design Changes	16	
4	Detailed Design	22
Parts & Materials	23	
Motor	23	
Gears	24	
Bearings	24	
Lead Screws	26	

Fasteners	26
Materials	27
Machining Methods	27
5 Conclusion	28
Bibliography	29
A CAD Renders	30
B Machine Drawings	40
C Product Specifications	43
D Photos	47

List of Figures

1.1	Early prototype of a static variable-friction shoe device by G. Millet [1]	3
2.1	Lead screw concept	8
2.2	Close up of the brake design	9
3.1	Compressive stress-strain curve of EVA foam (ZoteFoams)	13
3.2	The first iteration of the design	17
3.3	The gear train on the first iteration	18
3.4	Preliminary sketch of bearings	18
3.5	Drawing of the final bearing design for the rear brake	19
3.6	Second iteration showing addition of proper brake guides	20
3.7	Second iteration showing the change in the base and sides	20
3.8	Final iteration with the change to the back brake	21
3.9	Final iteration showing the detail of the back brake	21
4.1	Final Detailed Design	22
4.2	A look at the gear train	24
4.3	A close up of the bearings with the plate removed	25
4.4	A closer look at the bearing and circlips	26
A.1	Isometric overview	31
A.2	Isometric overview without the motor	31
A.3	Overview of the mechanism from the side	32
A.4	View of the side with the supports removed for viewing	32
A.5	Top view	33
A.6	Bottom with bearings visible	33
A.7	Bottom with no bearings	34

A.8 Close up of back brake	34
A.9 Back brake in down position	35
A.10 Back brake in up position	35
A.11 Close up of front brake	36
A.12 Front brake in down position	36
A.13 Front brake in up position	37
A.14 Isometric view from below	37
A.15 The rear brake system with brake guides	38
A.16 The rear brake system from the back	38
A.17 A close up of the bearings, gears, and circlip	39
A.18 A close up of the bearings, circlip, and gears, with the plate removed	39
C.1 Specifications of the NSK needle roller bearings	44
C.2 Specifications of the NSK radial flanged bearings	45
C.3 Moon's Industries 23HY9401 Pancake Super Flat 2-Phase Stepper Motor	46
D.1 Very preliminary sketch by G. Millet	47
D.2 Preliminary sketch of worm gear idea	48
D.4 Preliminary sketch of bearings	48
D.3 Preliminary sketch of lead screw idea	49

1

Introduction

The idea of developing variable-friction devices for friction-controlled walking has been researched and prototyped by the *Shared Reality Lab of the McGill Centre for Intelligent Machines* under the supervision of Professor Jeremy Cooperstock [1]. Their research has been into the development of a variety of actively controlled floor surfaces, including vibration-controlled friction, ball transfer units, and braking pins, as well as a vibrotactile shoe mechanism. This new design is of a shoe mechanism that uses a static slip surface and an active braking surface to vary the coefficient of friction on a specific passive floor surface.

Background

In the following explanation of the motivations behind the proposed work, the draft manuscript from a previous study is paraphrased, which includes some references to statistics concerning balance failures [1]. In the age group of those 65 years and older, falls are the cause of 88% of injuries [2], and can lead to their loss of independence and even death. It has been shown in Canada [2], the United States [3], China [4], and Finland [5], that one in three of those this age will fall once a year. Dealing with these injuries involves preventative measures, such as studying the way people walk and react to walking surfaces, as well as rehabilitation, like balance and mobility training. For rehabilitation training, simulated environments must be created to properly imitate the slip environments that cause people to fall. This requires the

control of such an environment, by creating a surface with a dynamic coefficient of friction, similar to a natural environment with real obstacles.

Designing a variable-friction walking surface has the potential to be useful in clinical or rehabilitation applications to simulate low-friction induced accidents. Research has been completed already to create a floor surface with very low coefficients of static friction, but has proven to be limited in supported footwear and in simulating natural walking patterns. The technology and expense behind creating a useful walking surface is also a limiting factor. By developing a shoe with the capabilities of varying the friction at the contact surface, more possibilities exist for floor types, and simulating natural walking becomes easier. The main challenge remains to be implementing the proper technology into the sole of a shoe, hence the inspiration for such a project.

Problem Definition

A lot of research has already been done to provide the resources for the design of a variable-friction shoe surface. Professor Cooperstock's lab has provided the foundation for this project with background information and even high-level concepts, off which a design can be based. They studied the mechanics behind natural human walking, regarding the forces of friction that cause slipping and how they can be controlled. The materials and methods that could be used for friction control were studied and design criteria defined.

The general concept for the design, created by Millet [1] over the past summer, involves varying the amount of contact between the floor and two shoe-surfaces of different coefficients of friction. One has a very low CoF, similar to that of ice, and the other a very high CoF. By varying the amount the high-friction surface protrudes from the low-friction surface, the weight distribution between the two surfaces changes, and this is proportional to the total effective friction force. When the translation of the high-friction surface is actively controlled, it acts like a brake, and the effective CoF, $\mu_{effective}$, can be varied dynamically while someone is walking. By introducing a sudden change in friction during a natural stride, a simulated slip environment is created. A fully static prototype of a shoe mechanism such as this was created and tested by Millet and is shown in Figure 1.1.



Figure 1.1: Early prototype of a static variable-friction shoe device by G. Millet [1]

The main challenge is to come up with a suitable mechanism that can carry out the necessary actions to successfully vary the friction, while satisfying the design requirements and fitting within the given constraints.

Design Requirements

To facilitate proper design, explicitly laying of the requirements of the design is a useful practice. As the design has evolved, the requirements have changed slightly, to reflect the focus of the actual prototype.

The device must:

- Contain one more mechanisms
- Be actively controlled
- Embed all mechanisms into the sole of a shoe
- Bear the load of a person on one surface
- Effectively change the friction coefficient of the shoe-ground interface

2

Conceptual Design

Working with Guillaume Millet, the Postdoctoral researcher who did the preliminary research on a mechanism that would fit into a shoe sole and consist of a passive low-friction surface and an active high-friction surface, we created some design criteria, generated possible concepts, analyzed the concepts and chose the best one.

Evaluation Criteria

In order to optimize the design, a set of criteria was created with which we could weigh and analyze the different concepts. This typically means maximizing efficiency, or increasing output and decreasing input. In this case, input is cost, weight, and complexity, and output is load and robustness. Additionally, and most importantly, the mechanism must be small enough to fit into the sole of a shoe and permit natural walking.

Cost

Something to always consider, while not a priority in this, is the cost and financial feasibility of the design. This design was budgeted at about \$350, and although not due to limited funds, it would not be practical to create a design much more expensive than this. When researching materials, components, and manufacturing methods, this must be considered.

Weight

As part of the design requirement that the mechanism permit natural walking, weight must be reduced as much as possible, as to not create an unnatural load on the user's feet. The target weight is set at 1kg per mechanism, as this is near to what a work boot weighs, which is the heaviest type of footwear the average person wears.

Complexity

Fewer moving parts and less complexity is almost always a goal in design, and in a design that must function and fit into the sole of a shoe, this is paramount. Moving parts mean space to move more degrees of freedom, which is difficult to implement in such a confined space. Additionally, the mechanism is required to hold the weight of a person, and a less constrained design means more places for failure.

Robustness

Stemming from the design requirement that the device must have a standing load of one person – about 700N - and handle the stresses of a person's stride, the design must be very robust. It needs to be able to use parts and materials that are strong enough to handle these loads, while still meeting the other requirements.

Size

The most important requirement is that the device is small enough to fit into the sole of a shoe. If the design cannot be made very small, than it is of no use, so size is the number one concern.

Concept Generation

Some concepts were suggested to me by Millet (Appendix D.1), and sketches were sent along with the ideas to begin the concept generation. The main principle of the concepts to be

generated is the method of turning rotational motion into vertical translational motion. A linear actuator is designed to do exactly this, but given the size requirements and custom geometry, this must be specially designed.

Wedges & Cable One idea is to utilize the mechanical advantage of two wedges, placed on top of each other, so that when they are forced inwards, they slide up each other's slope and cause an overall translation perpendicular to the input force. The input force would be driven by a motor, and converted to linear motion via a cable and system of pulleys.

Cam A similar idea to the wedge is to use a cam. The shape of a wedge essentially combines a cylinder with a ramp, so that rotational motion can easily be converted to translational motion, like in a car engine.

Worm Gear with Rack & Pinion Onto the idea of using gears, one method would be to drive a gear that spins a worm to transfer the rotational motion 90° , and then a rack and pinion to create the linear motion. A preliminary sketch of this can be found in Appendix D.2.

Lead Screw The other gear device involves one gear driving another gear, which is fixed to a lead screw. The lead screw is threaded into a lead nut, which converts the rotational motion to linear motion when its rotation is constrained (Appendix D.3).

Concept Evaluation

Wedges & Cable This concept excelled in the weight and cost criteria, as small cables and pulleys are much lighter and cheaper than cams and gears, but it lacked in robustness, simplicity, and size. Immediately, this seemed extremely difficult to implement on such a small scale, as cables need to be strong and tight, and their ductility becomes a large source of error when dealing with movements that are fractions of a millimeter. Additionally, the complexity of running cables through pulleys, securing them and calibrating the system is a large drawback.

Cam The cam idea is simple and elegant, assuming friction can be dealt with properly using a cam follower. The weight and cost are both also favorable. The weakness of this setup is the robustness. Having a cam and cam follower bear all the load of a person is not possible with the given geometry.

Worm Gear with Rack & Pinion While this seems like a good idea in theory, worm gears are only intended to be driven by the worm, not the gear. In order to achieve the proper motion, the geometry of the worm and gear setup would have to change dramatically, and this would reverse the gear ratio and render the mechanism useless.

Lead Screw Lead screws can be very robust, and are designed to handle a large static load because friction does not allow the force to be transferred to the gears. The gear train and motor laid sideways are very compact, and for the loads the mechanisms will have, the lead screw does not have to be large. This design is rather heavy, however, as it involves a lot of metal parts, which also makes it expensive. As far as complexity, it does have a lot of moving parts, but the implementation is straightforward, so it is neither a drawback nor an advantage.

Final Concept

The decision was made to go with the lead screw mechanism, for its robustness, and its ability to be implemented into such a small space. The complexity and weight are not favorable, but are of less importance, so they are a necessary deficiency of the design.

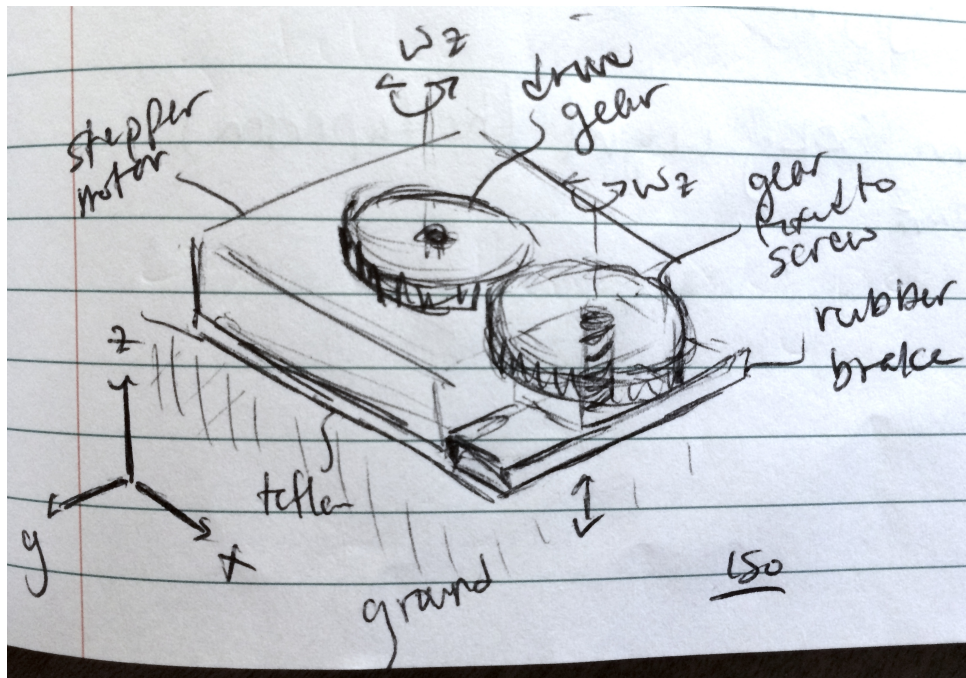


Figure 2.1: Lead screw concept

The idea of the lead screw design is to have a flat stepper motor fixed to a gear that drives a gear train as seen in Figure 2.1. The last gear in the train is fixed to a lead screw that is threaded into a plate, which acts as the lead nut. The plate is the base for a “brake,” which consists of a rubber sheet and a block of EVA foam. The whole “brake” is what translates vertically, as its rotation is constrained while being driven by the lead screw, just like a tube of deodorant (Figure 2.2). Surrounding this mechanism along the perimeter are supports that hold a thin strip of Teflon, or PTFE, that acts as the main contact with the ground. Both the mechanism and perimeter supports are attached to a base plate, which is shaped like the heel of a shoe, and provides support for the entire device. This plate is what is embedded into the sole of a shoe or boot, in place of the existing heel. Once this concept is prototyped, it should be simple enough to duplicate and add to the front of the shoe for full friction control.

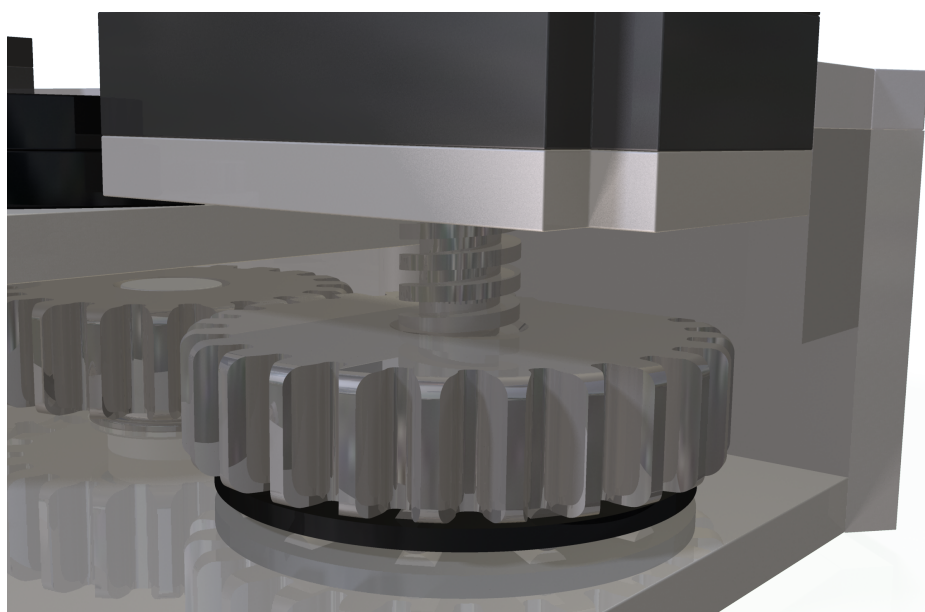


Figure 2.2: Close up of the brake design

3

Embodiment Design

After studying the work by Guillaume Millet, Martin Otis and Jeremy R. Cooperstock, and reviewing their equations, I had to do some calculations of my own. Once calculations were done, the proper sizes and dimensions were known, and the design began to fall into place. I based my initial vision of the device on what Millet had sketched and prototyped, and began designing the lead screw mechanism into that. As the design progressed, the most challenging part was satisfying the load and size requirements of the design. As more details were added for the sake of robustness, the size constraint became more important. In the end there were many iterations of the design, as necessary parts were added and the rest of the design would be altered to reflect those changes.

Guidelines & Previous Research

The first concept to understand when starting this design, is what “variable friction” actually means. Variable friction means simulating many different levels of static friction on a spectrum that ranges from normal contact friction between a rubber sole and the ground (about $\mu = 0.3$) to slipping on something as slippery as ice (about $\mu = 0.06$) [6].

Within this range, it is important to define the necessary step size needed to achieve a smooth, varying friction, based on the needs of the simulation. We have chosen to use ten different variations of friction in the range of $\mu = 0.06$ and 0.3 , with finer resolution as

friction approaches the slip condition (Table 3.1).

	μ
1	0.06
2	0.07
3	0.08
4	0.09
5	0.10
6	0.12
7	0.14
8	0.16
9	0.20
10	0.30

Table 3.1: Desired coefficients of friction (CoF)

How to achieve these coefficients The shoe sole is designed to incorporate a thin support with a slip surface that acts as the main contact surface, and an active brake mechanism as the secondary contact surface. Based off of the previous research, the ideal slip surface is Teflon, or PTFE, as its self contact friction, μ_S , is about 0.05 [1]. The high friction surface should be rubber, in an attempt to reach $\mu = 0.5$, as this is the CoF of rubber on dry asphalt – a typical surface for a shoe. The active brake mechanism, with the rubber surface, is extended beyond the surface of the Teflon, so that both the Teflon and rubber make contact with the ground. Underneath the layer of rubber, the brake also has an elastic material. This elastic material allows the brake to deform when it makes contact with the ground, and it deforms until it is flush with the Teflon surface. As force is proportional to deformation, as shown in the next section, the more the brake deforms, the more force is exerted on it. This force is what determines the amount of friction force that is delivered by the shoe, and in turn controls the effective coefficient of friction. To determine exactly how to dynamically accomplish this with a mechanism, some calculations must be made.

Calculations

To begin, we look at the underlying mechanics of what is going on at the brake, in general terms. The force of friction acting on one rubber brake is a product of the CoF of the rubber and the normal force from the human that is being transmitted to the brake as in Equation 3.1. It is this friction force that is ultimately being controlled.

$$F_{friction}^{brake} = \mu_{rubber} F_{human}^{brake} \quad (3.1)$$

Additionally, the force from the human causes a strain proportional to the Elastic Modulus of the brake material, causing the brake to deform quite a bit.

$$F_{human}^{brake} = \frac{E_{brake} S_{brake} \Delta L}{L} \quad (3.2)$$

When the deformation, ΔL , is limited to the length of protrusion of the active brake mechanism, only the F_{human}^{brake} that satisfies this equation will be transmitted through the brake. The rest of the force of the human will be supported by the slip material around the edges, and it is this relationship between the force on the brake and the slip surface that varies the friction. This is shown in Equation 3.3 given by Millet, Otis and Cooperstock [1].

$$F_{human} = F_{lowfriction} + F_{highfriction} \quad (3.3)$$

Equation 3.2 can be rewritten more generally as

$$F_{highfriction} = E_{elastic} S_{elastic} \varepsilon_{elastic} \quad (3.4)$$

and combined with Equations 3.3 and 3.1 to give the relationship between the coefficients of friction, and how the effective CoF is achieved (Equation 3.5).

$$\mu_{effective} = \mu_{lowfriction} + (\mu_{highfriction} - \mu_{lowfriction}) \frac{E_{elastic} S_{elastic} \varepsilon_{elastic}}{F_{human}} \quad (3.5)$$

where F_{human} is the vertical force applied on the shoe, $F_{lowfriction}$ is the normal force on the low friction surface, $F_{highfriction}$ is the normal force on the high friction surface, $E_{elastic}$

is the Young's Modulus of the elastic element, $\varepsilon_{elastic}$ is the controlled deformation of the elastic material, $S_{elastic}$ is the surface area of the high friction surface, and $\mu_{lowfriction}$ and $\mu_{highfriction}$ are the respective coefficients of friction.

Using Equation (3.5) and assuming $E_{elastic}$, $S_{elastic}$ and F_{human} to be constant, we can solve for $\varepsilon_{elastic}$ or ΔL for each desired $\mu_{effective}$. This will give us the required deformation, and therefore translation, needed to vary the friction by the desired amount.

The problem with this, however, is that these values are not constant. Both $S_{elastic}$ and F_{human} vary with stride, and $E_{elastic}$ for the EVA foam elastic material can only be considered linear in the first 40% of deformation, as shown in Figure 3.1.

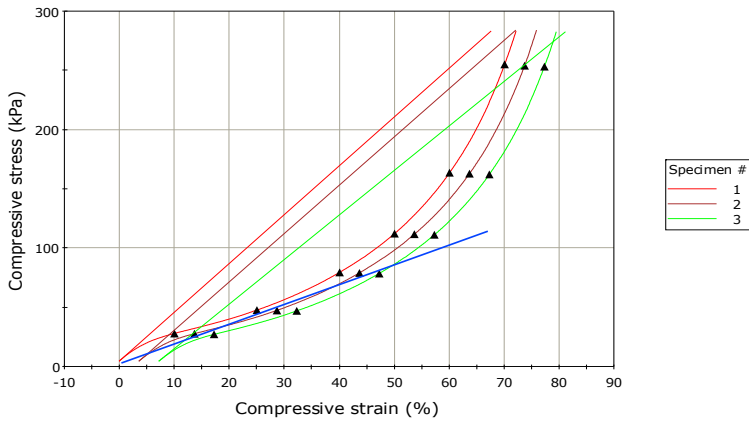


Figure 3.1: Compressive stress-strain curve of EVA foam (ZoteFoams)

To get around these issues and get an estimate, we consider only the linear region of the elastic material, as the small deformations ($\varepsilon_{elastic} < 40\%$) are what result in the lowest friction coefficients, and this is where the resolution is the smallest. At full brake extension, the elastic material can deform up to 80% (See Appendix A.10 for a visual of total brake extension) and at this strain, the Elastic Modulus becomes very high. The resolution for controlling the strain becomes large here, but precision is not needed.

Regarding the change in force and surface area over a stride, we can choose reasonable values for the calculations, but for proper testing, a force-torque sensor will be placed into the brake pad. The sensor will be able to sense when there is a load on that particular brake, which will give a nominal surface area (Equation 3.6) and a force reading. These readings will not necessarily be used in real time, but will at the very least make it possible to calibrate the device.

Total effective surface area given by:

$$S_{elastic, \text{effective}} = \sum_{i=1}^n S_{elastic, i} \quad (3.6)$$

where n is the number of elastic elements and $S_{elastic} > 0$ if $F_{human} > 0$, as sensed by the F-T sensor.

To calculate the necessary resolution of the brake, we will consider the minimum load spread over the most area, for the least strain and therefore smallest resolution. The Elastic Modulus to be used will be 80kPa, as reported by G. Millet [1], and the $S_{elastic}$ and F_{human} will be chosen to be the the surface area of two braking surfaces as shown in Equation 3.6 – totaling $0.00115m^2$ – and a F_{human} of 350N – an average weight of a human on one shoe. Of course the actual value of $E_{elastic}$ will have to be tested for and the device calibrated, and proper force readings will be taken from the F-T sensors.

$$\varepsilon_{elastic} = \frac{(\mu_{effective} - \mu_{lowfriction})}{(\mu_{highfriction} - \mu_{lowfriction})} \frac{F_{human}}{S_{elastic} E_{elastic}} \quad (3.7)$$

Let's use:

$$\mu_{low \ friction} = 0.05$$

$$\mu_{high \ friction} = 0.30$$

$$E_{elastic} = 0.080 \text{ MPa} [1]$$

$$F_{human} = 350 \text{ N}$$

$$S_{elastic} = 0.00115m^2 [20mm \times 30mm + 55mm \times 10mm]$$

$$\text{and } \mu_{effective} = [0.06, 0.07, 0.08, 0.09, 0.10, 0.12, 0.14, 0.16, 0.20, 0.30] \quad 3.1$$

Putting this into MATLAB we get:

```
>> strain_resolution
```

```
strain =
```

0.1458	0.2917	0.4375	0.5833	0.7292	1.0208	1.3125
1.6042	2.1875	3.6458				

The results show that over 100% strain would be needed to achieve a $\mu_{effective}$ of 0.12,

which of course is impossible. This is due to the nonlinear elastic property of the material being modeled as linear. At this $\mu_{\text{effective desired}}$ and higher, the strain will certainly be nonlinear, and need to be calibrated manually through testing. The important results from this are the strains closer to the slip condition.

The resolution needed is the difference between these smallest strain values:

$$\Delta\varepsilon_{\text{elastic min}} = |\varepsilon_{\text{elastic}}^{\mu=.06} - \varepsilon_{\text{elastic}}^{\mu=.07}| \quad (3.8)$$

where the necessary travel of the brake is ΔL given by:

$$\Delta L = \varepsilon_{\text{elastic min}} L \quad (3.9)$$

For $L = 6\text{mm}$ as defined by the thickness of the EVA foam, the minimum resolution ΔL is 0.8748mm .

This seems like a very small increment, but what is important is that the gear ratio, lead screw and stepper motor can make this small of a change. To begin, we start with the minimum rotation of the stepper motor, as this is the limiting factor. Equation 3.10 shows the minimum step size of the motor, as given by the manufacturer, to be 1.8° .

$$\theta_D = 1.8^\circ = \frac{1.8^\circ}{360^\circ} 2\pi = 0.0314 \text{ rad} \quad (3.10)$$

where θ_D is the step size of the stepper motor, or the minimum rotation of the driving gear. The rotation of the active gear is then just a function of the gear ratio:

$$\theta_{\text{active}} = \theta_D \frac{R_D}{R_{\text{active}}} \quad (3.11)$$

where we neglect the intermediate gear, since the ratio between the driving gear and the intermediate gear is 1:1.

Without choosing the lead screw first, we can calculate the pitch angle that would be needed to attain the desired resolution in one step of the motor.

$$\phi_{\text{pitch}} = \tan^{-1}\left(\frac{\text{min resolution}}{\text{arc length of screw}}\right) = \tan^{-1}\left(\frac{\text{min resolution}}{\theta_F R_{\text{lead screw}}}\right) \quad (3.12)$$

With a min resolution of 0.8748mm and $R_{\text{lead screw}} = 2.41\text{mm}$, the ϕ_{pitch} is 86.06° . This

maximum angle is much higher than the standard angle of a lead screw ($3^\circ - 6^\circ$), which means much more precision can be achieved by using a smaller pitch angle and having the motor spin many more times than the minimum step size. A few revolutions of the motor per minimum resolution means more fine tuned control at little cost.

By choosing a lead screw with the smallest lead makes the resolution smaller, and the friction lower. Using a 1mm lead and having a $R_{lead\ screw}$ of 2.41mm, the ϕ_{pitch} is 3.79° .

Based on the choice of lead screw, the number of revolutions of the motor per resolution step can be calculated. The angle of the lead screw is $\phi_{lead} = \tan^{-1}\left(\frac{lead}{\pi D}\right)$ and for the desired resolution, the angle of rotation of the lead screw and gear is $\theta_{active} = \frac{lead_{desired}}{\tan\phi_{lead}R_{lead\ screw}}$. Using the gear ratio, as in Equation 3.11, it is clear that the driving gear and stepper motor must then turn $\theta_D = \theta_{active}\frac{R_{active}}{R_D} = 5.496\ rad$ or 314.9° to deliver the translational motion of one resolution to the braking surface. This means that the motor turns nearly one full revolution to deliver one change in resolution to the brake, which means excellent precision can be attained.

Design Changes

The current design went through many iterations to get it right. Of course the original design will not work perfectly, so after reviewing the concept with Guillaume Millet and Professor Cooperstock many times, the design evolved and improved.

First Iteration The first design consisted of only three gears, one driving and two active, with a much larger gear ratio. This gear ratio allowed for more precision in the brake, but still met the size constraints. The bearings chosen at this stage were simply thin faced axial thrust bearings, with no radial bearings. The base plate and side supports were curved to fit the shape of a shoe heel, and there were only some very small guide pieces to constrain the rotation of the brakes. This iteration can be seen in Figure 3.2 and is clearly an unfinished design.

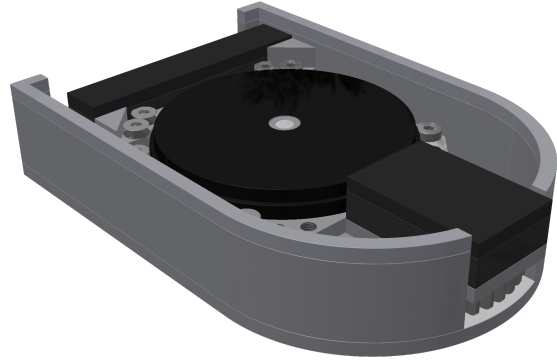


Figure 3.2: The first iteration of the design

After showing the design to the supervisors, some criticisms were made, which required some redesign.

First, the way the gears were set up, required the lead screw to pass through the rear brake asymmetrically, which would create a large torque on the screw, gear and base. This had to be redone somehow. The solution to this was to rethink the gear train, so that the gears could be centered directly underneath the brakes. This meant adding a set of intermediate gears to push the centers of the lead screws farther apart and allow for this geometry. This would in turn change the gear ratio and add more complexity, but it had to be done. In place of the 45-tooth gears that were originally there – see Figure 3.3 – two 20-tooth gears were added, and then two 25-tooth gears became the active gears. The gear ratio changed from 20:45 to 20:25, but after redoing the calculations, the change was not major.

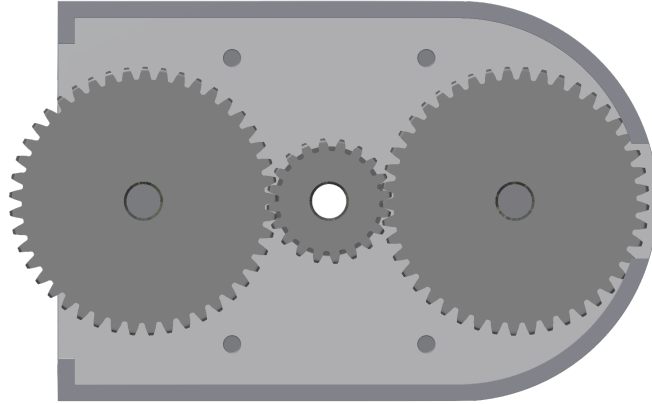


Figure 3.3: The gear train on the first iteration

Additional to the uneven loading of the brake was the consideration that there will be some tangential forces on the brakes that will cause a moment regardless of symmetry. This meant that the joints would have a radial load, not just an axial load as I had assumed. The answer to this was to come up with some bearings that could handle this. Some sketches were made to model the forces and we came up with a setup that required two bearings and an extra bracket (Figure 3.4). After designing this, it was clear that it would be much too thick, and an alternative was considered. The alternative was to use an angular contact bearing that could handle both axial and radial loads. This proved to also be too thick.

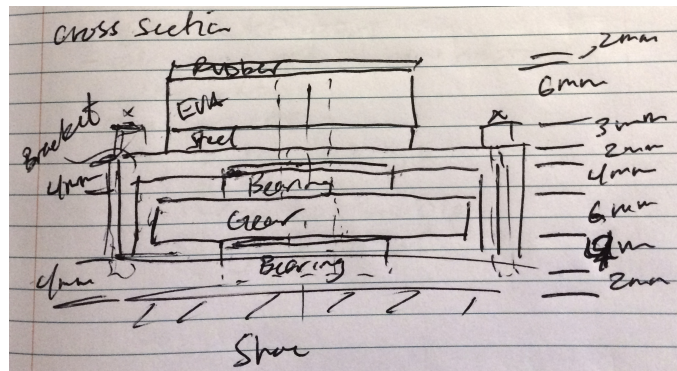
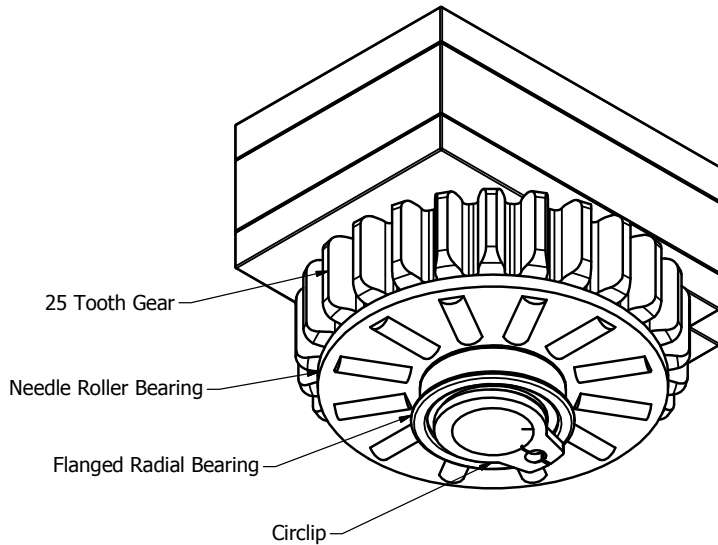


Figure 3.4: Preliminary sketch of bearings

The design that in the end would be successful involves one flanged radial ball bearing that fits in from the other side of the base plate and a needle roller bearing that fits around the radial bearing on top of the plate. As seen in Figure 3.5, the hub that runs through the

bearings is held in place with a circlip, or external retaining ring, which just keeps it from falling out due to gravity. With this setup, all the fits are slightly loose, so that the axial loads are transferred into the roller bearings and the radial loads into the ball bearings. This ensures that the system is not over-constrained.



Iso Below

Figure 3.5: Drawing of the final bearing design for the rear brake

Second Iteration The second iteration involved adding guides for the brakes so that their rotation was constrained properly and that the friction between the brake plates and the surrounding components was not an issue. Custom aluminum pieces were designed to attach to the base plate and rest flush with the brake so that when it translated, it was guided by this part.

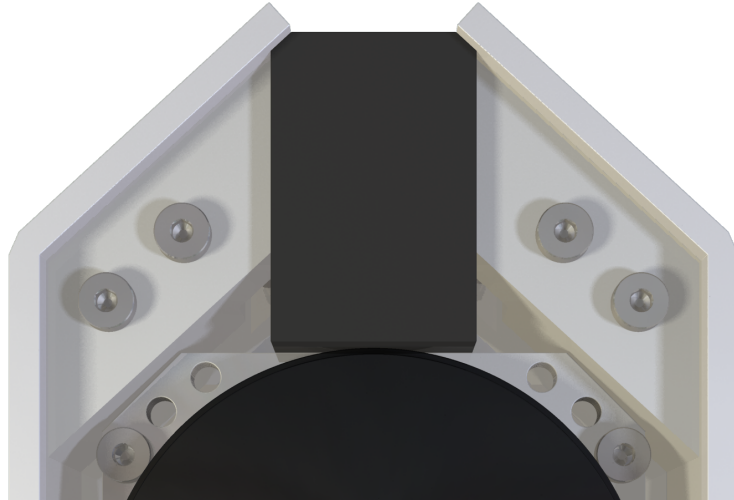


Figure 3.6: Second iteration showing addition of proper brake guides

In addition to this, the manufacturing methods were reexamined, and it became clear that the base plate and side supports would be difficult to machine into the curve shape, and this was an unnecessary feature. They were redesigned to just include one angle that would match the shape of of a shoe close enough to not be an issue, but make the machining and assembling much easier. Fasteners were also added in this iteration, as seen in Figure 3.7.

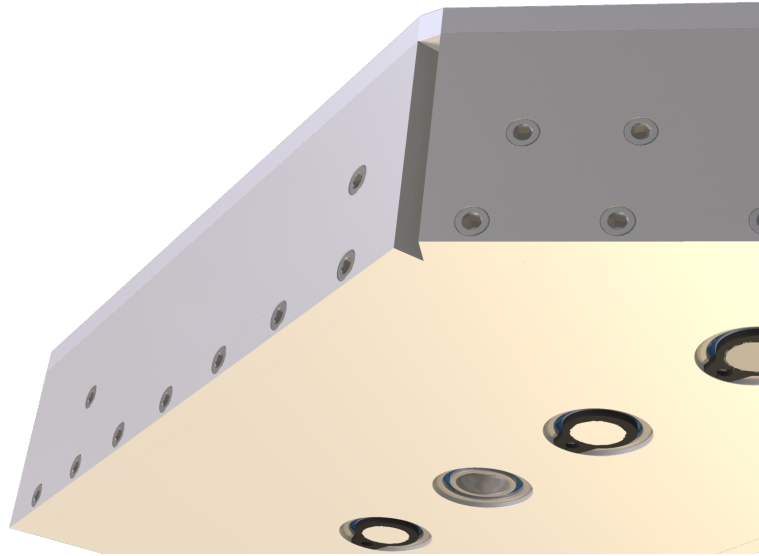


Figure 3.7: Second iteration showing the change in the base and sides

Final Iteration The final design made minor changes to the rear brake to address some issues that the heel strike would cause a large tangential force on the brake that would cause too much deformation towards the back of the device. To solve this, the supports and guides were changed so that the leading edge of the heel would have a better balance of Teflon and rubber. This would add support when the shoe strikes the ground, so that it doesn't torque on the brake too much. Figures 3.8 and A.16 show this part of the final design.

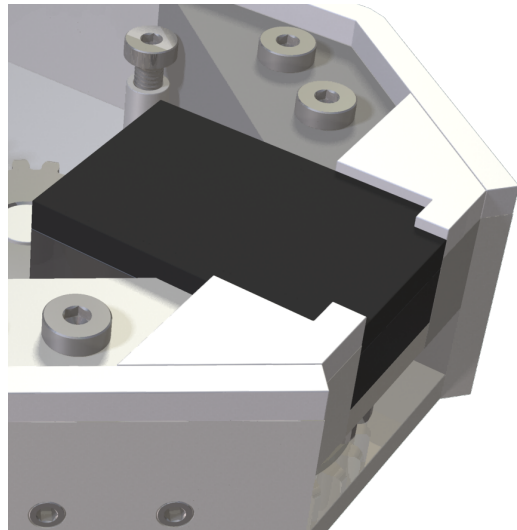


Figure 3.8: Final iteration with the change to the back brake

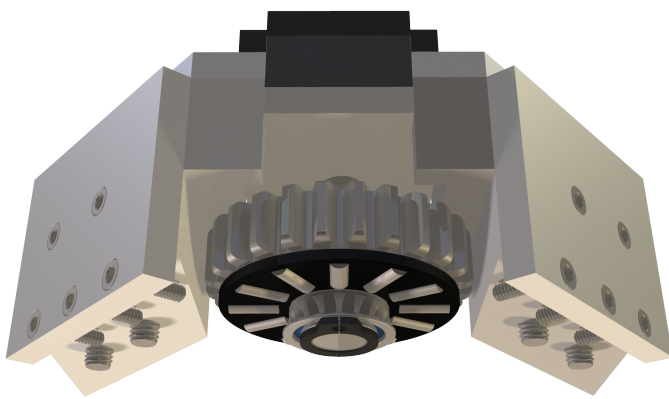


Figure 3.9: Final iteration showing the detail of the back brake

4

Detailed Design

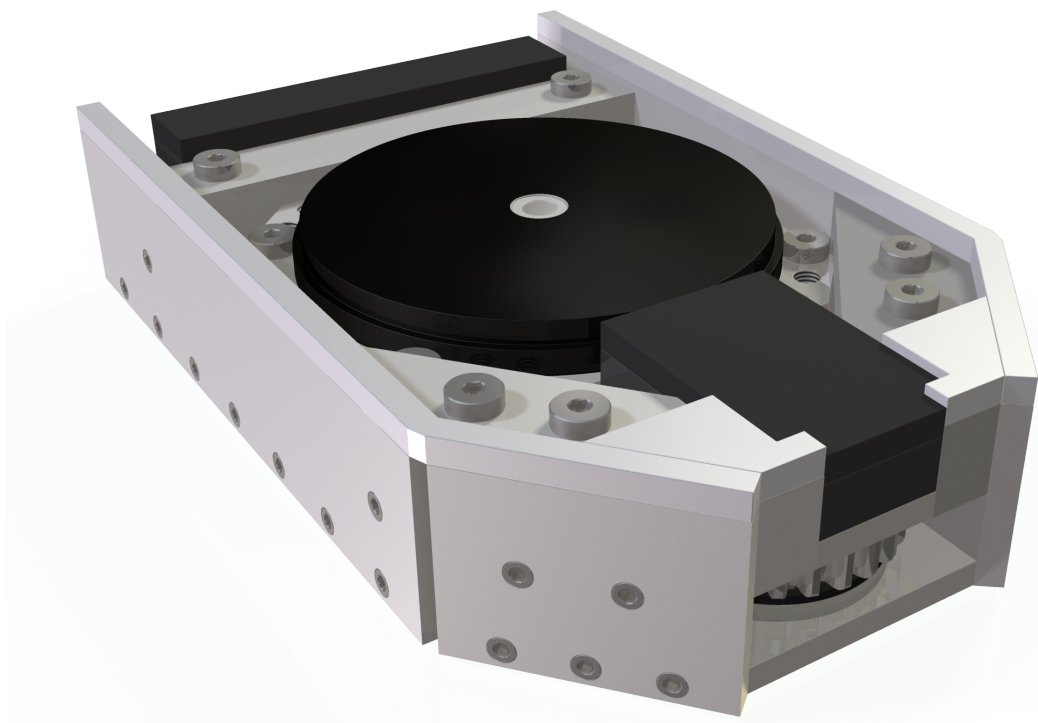


Figure 4.1: Final Detailed Design

The final design consists of five gears, five radial bearings, five circlips, two needle roller bearings, seven spacers, two hubs, two lead screws, seven steel plates, two EVA foam pieces, two rubber sheets, four PTFE sheets, three aluminum blocks, one motor, and thirty eight bolts. These parts make up the base plate, the supporting edges, the gear train, and front and rear brakes. The final detailed design takes into account the stresses on the brakes and edges, the friction in the gears, lead screws, and brakes, the material properties, the manufacturing of the parts, and the performance of the motor. After many calculations and a few iterations of design, the parts and materials are ready to be ordered. CAD renders in Appendix A show the many angles of the finished design, and drawings in Appendix B give details of how the device works.

Parts & Materials

The device has been entirely designed with the choice of materials and parts in mind. When designing any device, it is important to always find sources for all the parts and materials that are required, as knowing what must be fabricated and what can be purchased weighs heavily on the success of the design. In the case of a mechanism such as the variable friction shoe surface device, sourcing components is especially difficult due to the size and load requirements. Some of the iterations of the design were made due entirely to the choice of parts. In the next section, the details of all the parts are laid out.

Motor

The motor was chosen to be a pancake stepper motor, which is a hybrid brushless DC motor that moves in small increments of 1.8° . This style of motor runs off of DC voltage, has closed loop, yet very precise, rotation, and a high power density. The specific choice is the Moon's Industries 23HY9401 Pancake Super Flat 2-Phase stepper motor, that is only 9mm thick and a 55mm square profile (Appendix C.3). It weighs just 80 grams. The motor shaft is 6mm in diameter, which will be fit into the hubless drive gear.

Gears

The gear train is made up of five gears; one drive gear with an intermediate gear on each side, and then an active gear outside each of those. The drive and intermediate gears are both 20-tooth gears, and the active gears on the outside are 25-tooth. This creates a gear ratio of 20:25 or 4:5, which gives the active gear less torque and slower motion. The gears being used come from [Quality Transmission Components](#) and are models SSAY1-20 and SSAY1-25. These models are steel, hubless, thin face spur gears and are only 6mm thick with pitch diameters of 20mm and 25mm respectively. They each weigh about 15 grams. Figure 4.2 shows the gear train from the bottom, with the plate and bearings removed.

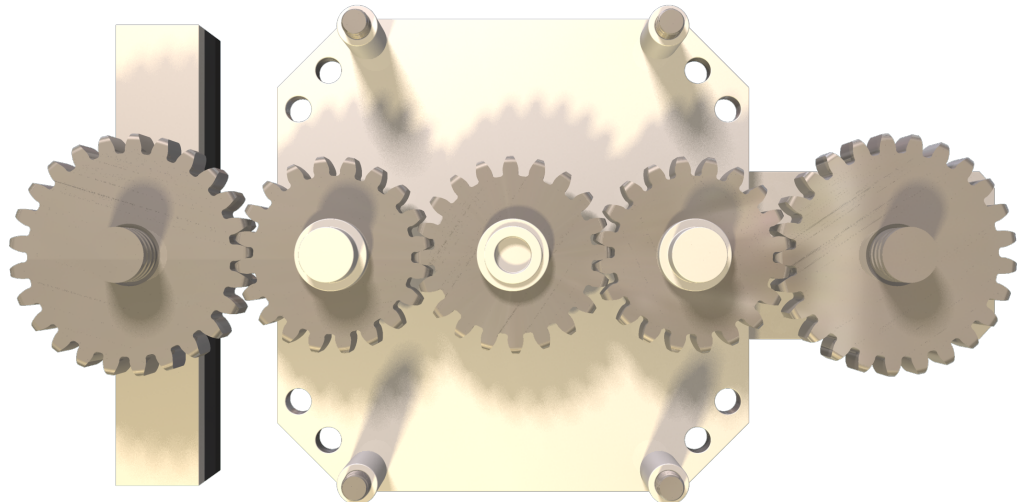


Figure 4.2: A look at the gear train

Bearings

Two types of gears are used to allow movement with both axial and radial forces being exerted on the rotating parts. The two brakes are taking all the stress and most of that is in the axial direction, so they need bearings that can take this load. The axial load bearings chosen are NSK Thrust Needle Roller Bearings, with a very small thickness. They have an

I.D. of 10mm, O.D. of 24mm and thickness of 2mm, but can handle axial loads up to 7700N. These are the black bearings visible in Figure 4.3.

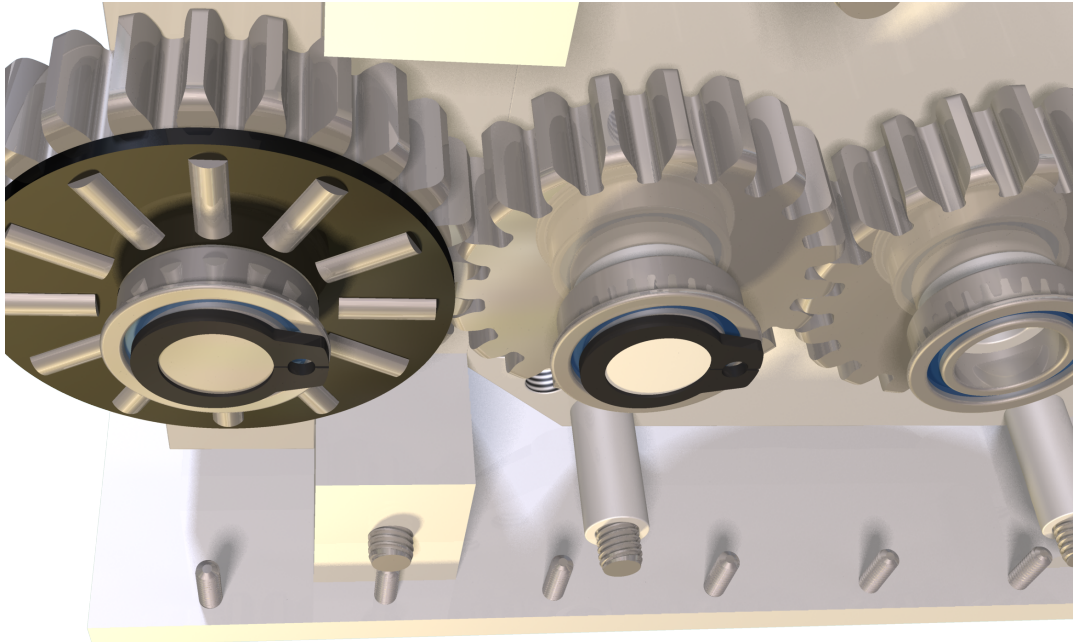


Figure 4.3: A close up of the bearings with the plate removed

The radial bearings are needed for all the gears to allow free rotation, and are chosen to be flanged so they can be attached from the other side of the base plate. Specifically, they are [NSK Miniature Flanged Single-row Deep Groove Ball Bearings](#) and have an I.D. of 6mm, O.D. of 10mm, and thickness of 3mm with the flange. They can still bear a radial load of up to 495N as shown in the spec sheet in Appendix C.2.

The shaft that runs through the radial bearings is then held into place by a 6mm circlip that can be found through McMaster. The [Steel External Retaining Ring](#) can take no load, but simply keeps the shaft from falling through. The bearings and circlip can be seen up close in Figure 4.4.

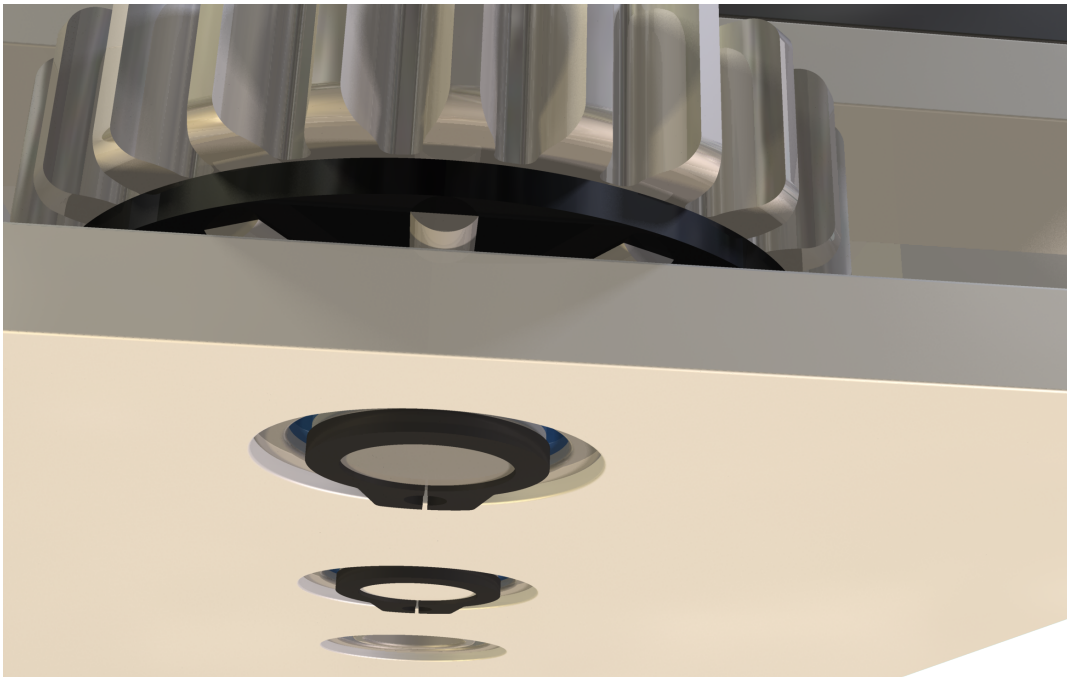


Figure 4.4: A closer look at the bearing and circlips

Lead Screws

One lead screw on each brake is what drives them upwards and bears the load of the person. Fortunately, a 6mm lead screw is very strong, with a plastic nut typically good for 100lb, so with a custom, steel lead nut, the system should be robust enough to meet the requirements. The lead screw will be a [Kerk Acme Rolled Stainless Steel Lead Screw](#) with a 6mm diameter, cut to 20mm, with a special order lead nut, provided by Kerk as well. This combination should have a lead accuracy of .0001mm/mm, which means the resolution needed to attain our coefficients of friction will not be affected.

Fasteners

All bolts were chosen to be stainless steel, metric, low head, socket cap screws for standardization and ease of assembly. Only one tool should be necessary to change all the bolts. All the bolts, except those that hold the side supports to the base are M3 bolts of varying length and are purchased from [McMaster](#). The smaller bolts are M1.6 and are also found

on McMaster. No nuts were used, as all the screws should be threaded right into the base or corresponding part, which means that all the holes will have to be tapped.

The screws that hold the motor will need plastic spacers to lift the motor off the base plate the appropriate amount, and the three intermediate gears need thin spacers to align them with the active gears. These spacers are also standard parts available from McMaster, and will be ordered with the fasteners.

Materials

The base plate, side supports, and brake guides will all be machined out of aluminum plates of varying thicknesses. The bottom plate and the side supports are made from a 3mm thick plate, while the brake guides will need to be machined from a block with a 20mm × 20mm profile.

The Teflon PTFE and gum rubber will be cut from a 3mm thick sheets and the EVA foam from a 6mm sheet. These are all standard materials and thicknesses that can be sourced from McMaster.

Machining Methods

Some parts will need to be machined, and this has been considered in the design. The base plate is not too complicated, with angles cut from the corners and a few holes in a line down the middle. The side supports are simply rectangles with some holes drilled and countersunk. The only challenge is the brake guides, which involve some more advanced milling in the angles and cut-aways, but should still be able to be done in a conventional mill.

5

Conclusion

After an initially easy decision on which concept to design, the minor details became the real extent of the design process. Making a device that fits into a shoe is no easy feat, and the bulk of the research and design went into finding the right components and configurations to fit the size and load requirements. The final model reflects numerous calculations, hours of research, and many iterations of design.

The next step is to review the machine drawings and begin ordering parts and materials. This step can be done in early January so manufacturing can begin by the end of the month. Assembly should take about another couple weeks, and this leaves at least a month to test and redesign if necessary.

Bibliography

- [1] G. Millet, M. Otis, and J. R. Cooperstock, “Variable-friction devices for friction-controlled walking.” Unpublished.
- [2] V. Scott, L. Wagar, and S. Elliott, “Falls & related injuries among older canadians: fall-related hospitalizations & intervention initiatives,” tech. rep., Public Health Agency of Canada, 2010.
- [3] J. M. Hausdorff, D. A. Rios, and H. K. Edelberg, “Gait variability and fall risk in community-living older adults: A 1-year prospective study,” *Archives of Physical Medicine and Rehabilitation*, vol. 82, no. 8, pp. 1050 – 1056, 2001.
- [4] L.-W. Chu, I. Chi, and A. Chiu, “Incidence and predictors of falls in the chinese elderly,” *Annals, Academy of Medicine, Singapore*, vol. 34, no. 1, pp. 60 – 72, 2005.
- [5] H. Luukinen, K. Koski, L. Hiltunen, and S.-L. Kivela, “Incidence rate of falls in an aged population in northern finland,” *Journal of Clinical Epidemiology*, vol. 47, no. 8, pp. 843 – 850, 1994.
- [6] A. Roberts and J. Richardson, “Interface study of rubber-ice friction,” *Wear*, vol. 67, no. 1, pp. 55 – 69, 1981.

Appendix A

CAD Renders

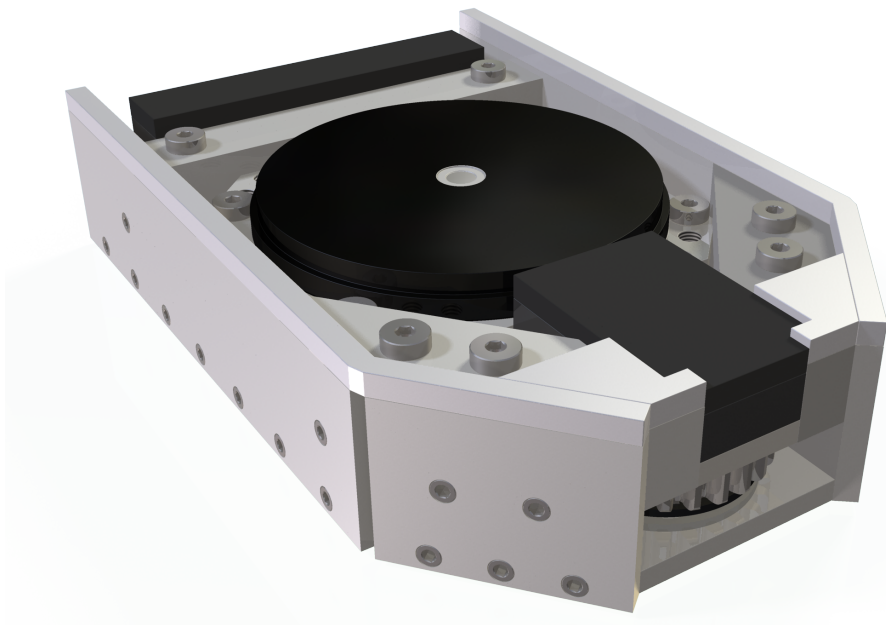


Figure A.1: Isometric overview

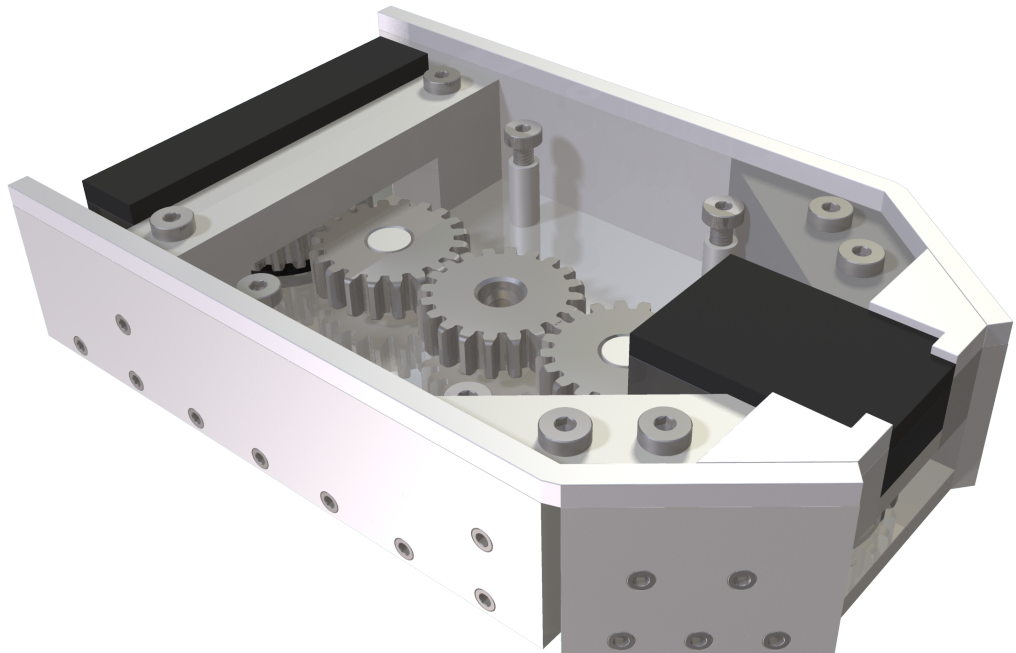


Figure A.2: Isometric overview without the motor

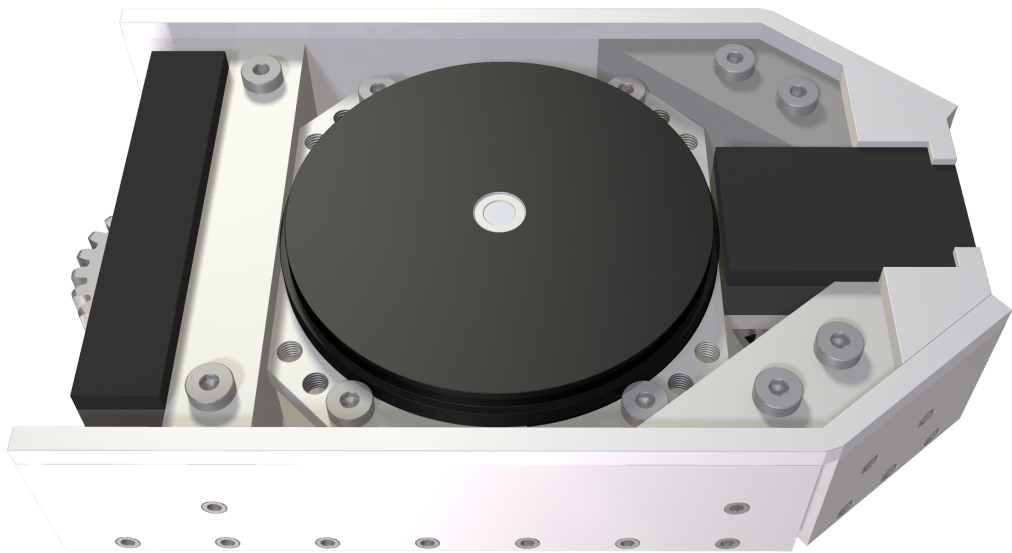


Figure A.3: Overview of the mechanism from the side

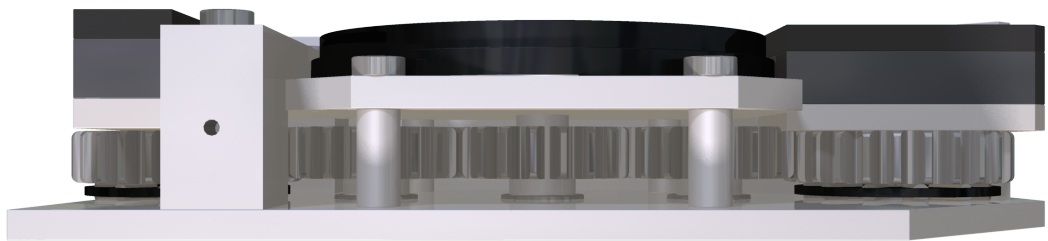


Figure A.4: View of the side with the supports removed for viewing

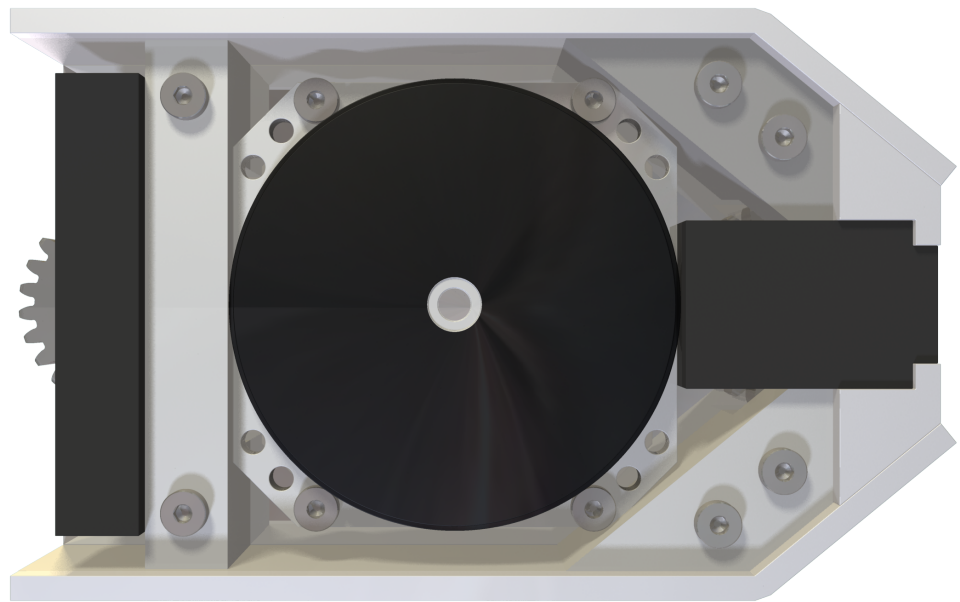


Figure A.5: Top view

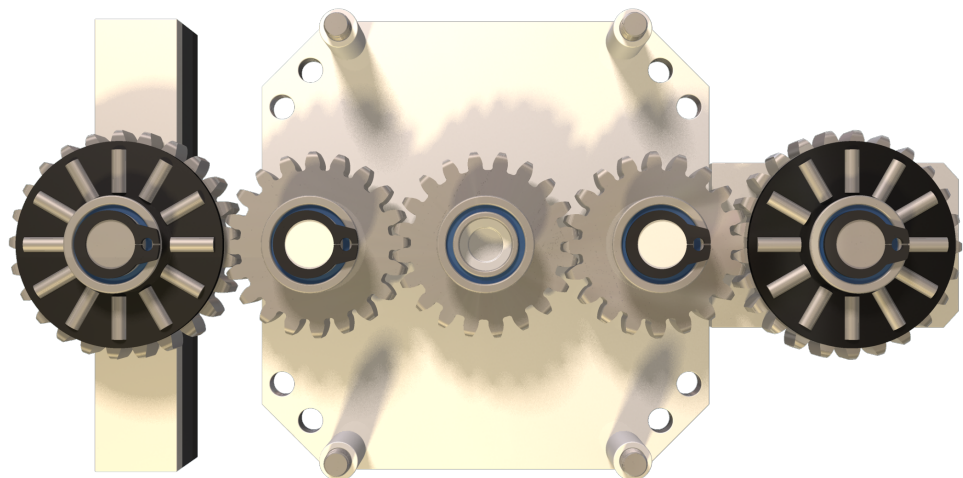


Figure A.6: Bottom with bearings visible

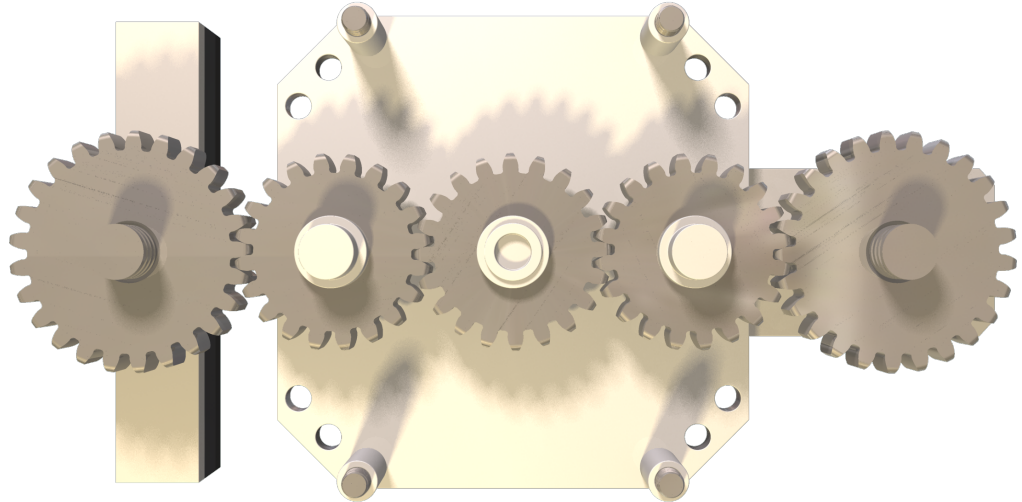


Figure A.7: Bottom with no bearings

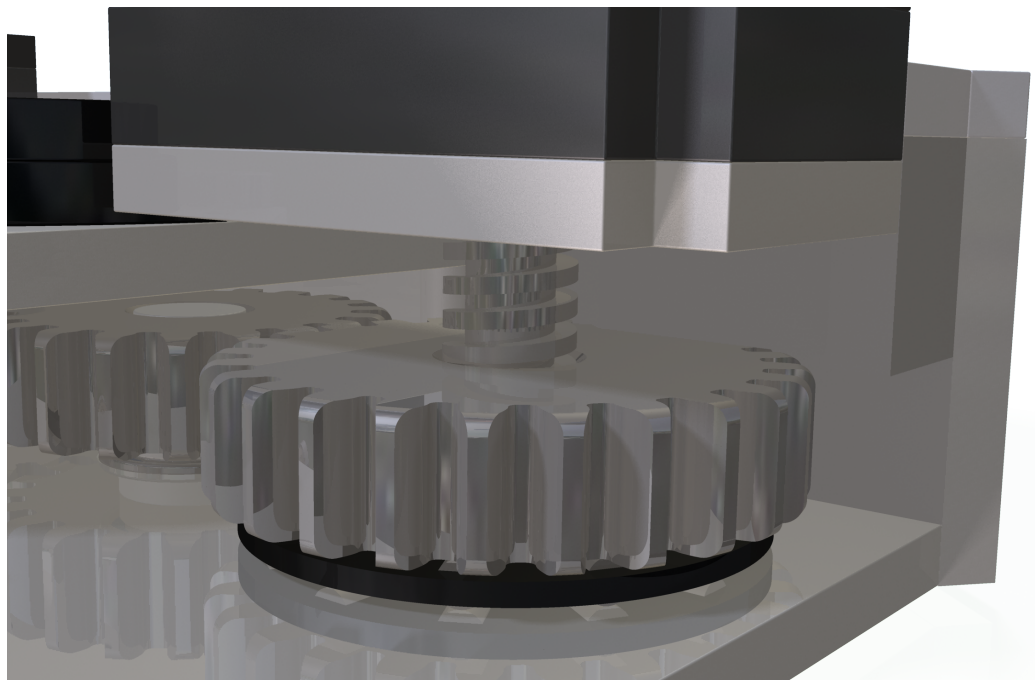


Figure A.8: Close up of back brake

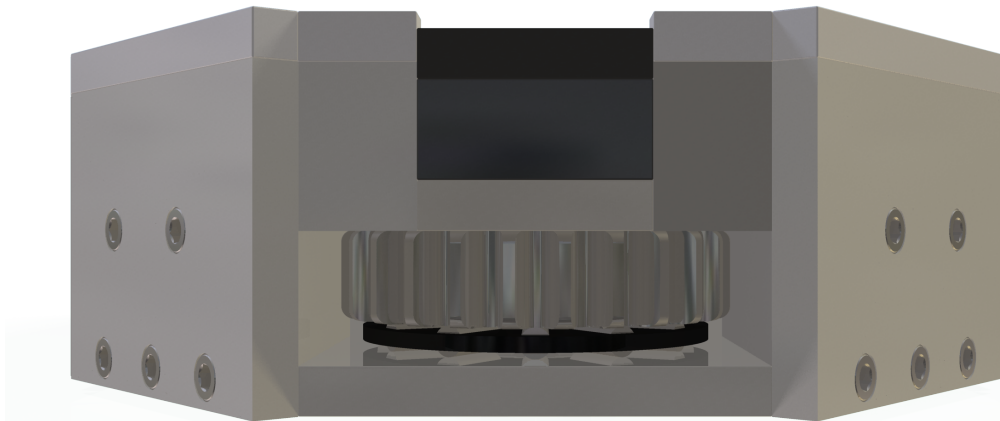


Figure A.9: Back brake in down position

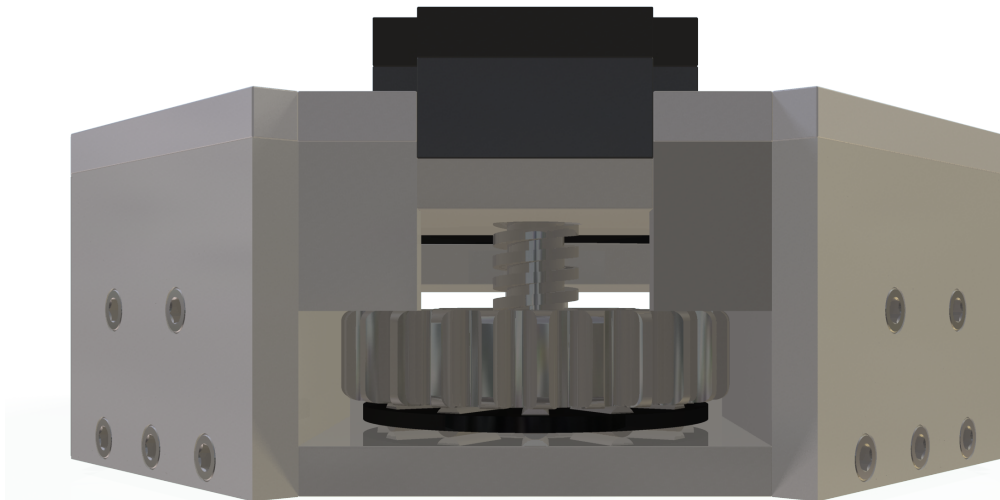


Figure A.10: Back brake in up position

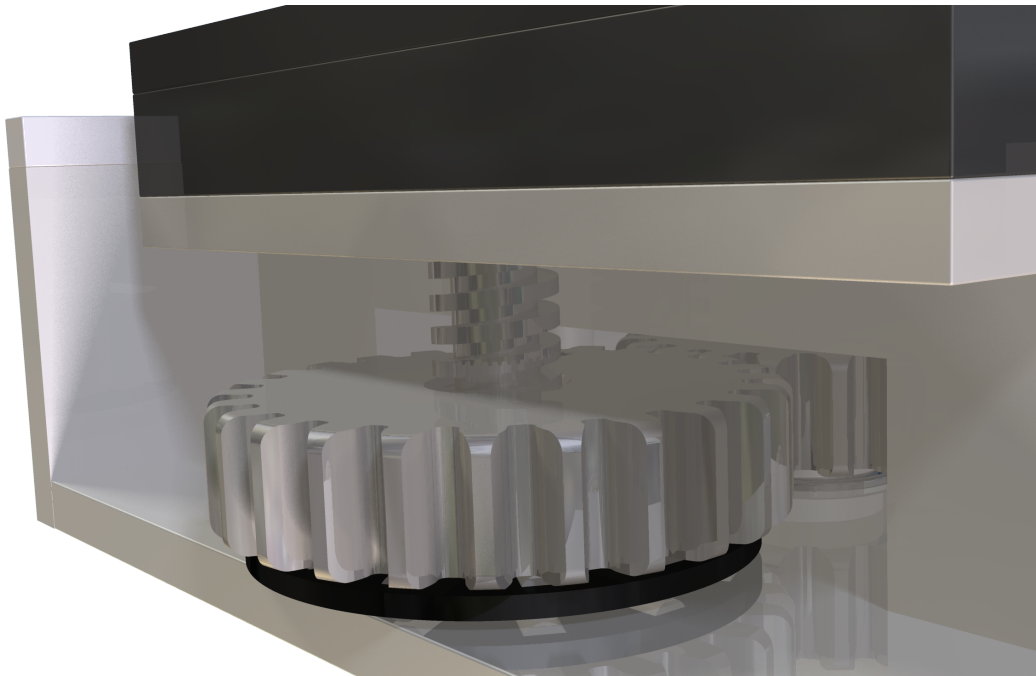


Figure A.11: Close up of front brake



Figure A.12: Front brake in down position

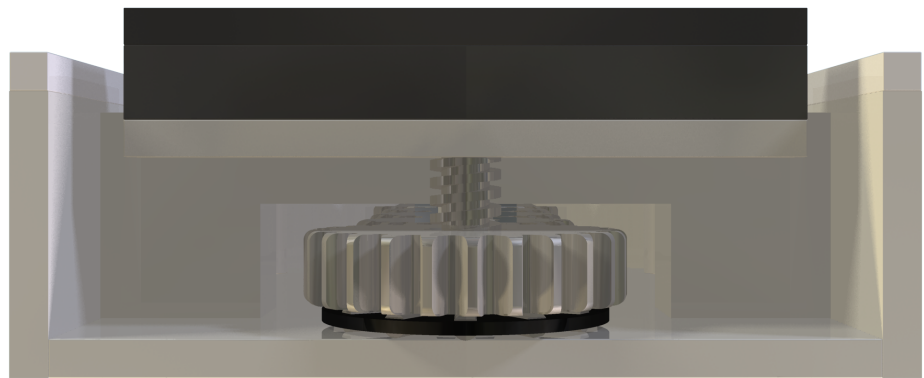


Figure A.13: Front brake in up position

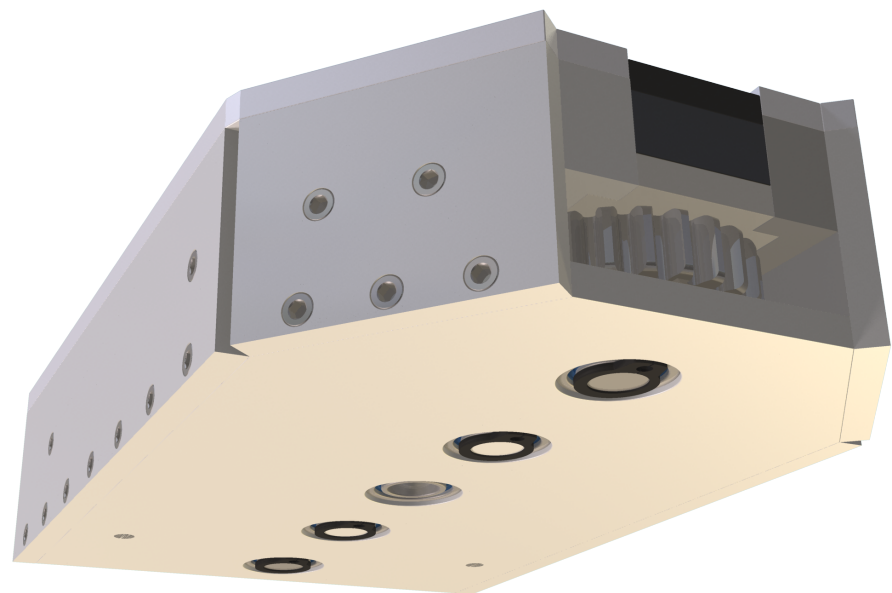


Figure A.14: Isometric view from below

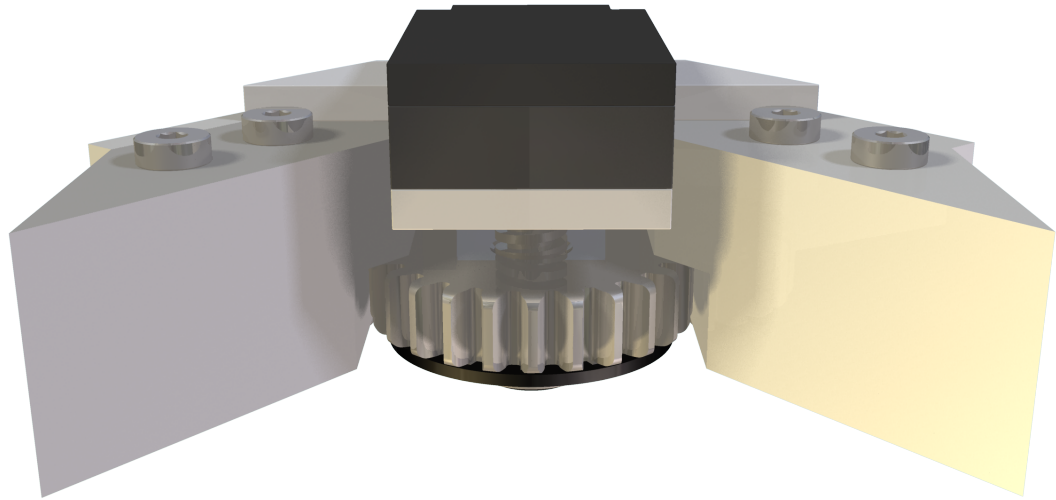


Figure A.15: The rear brake system with brake guides

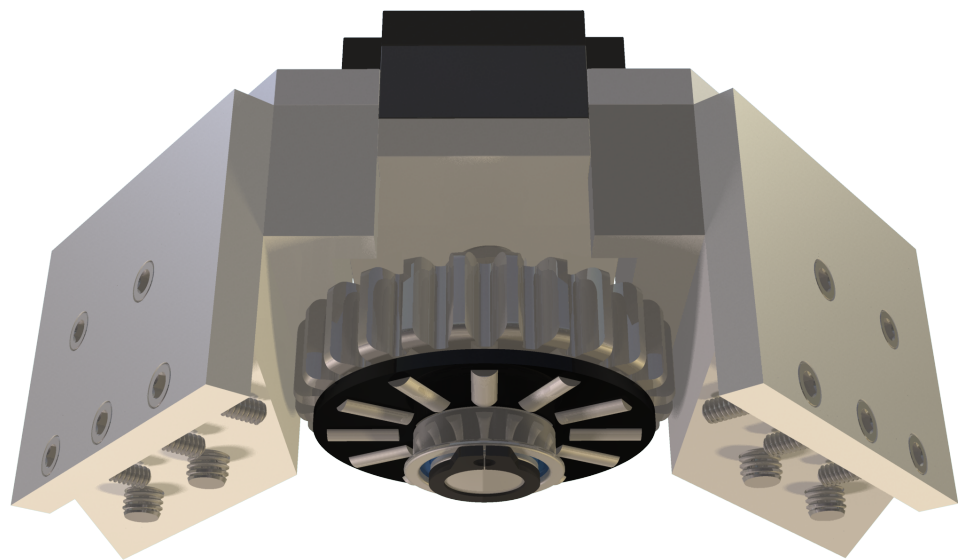


Figure A.16: The rear brake system from the back

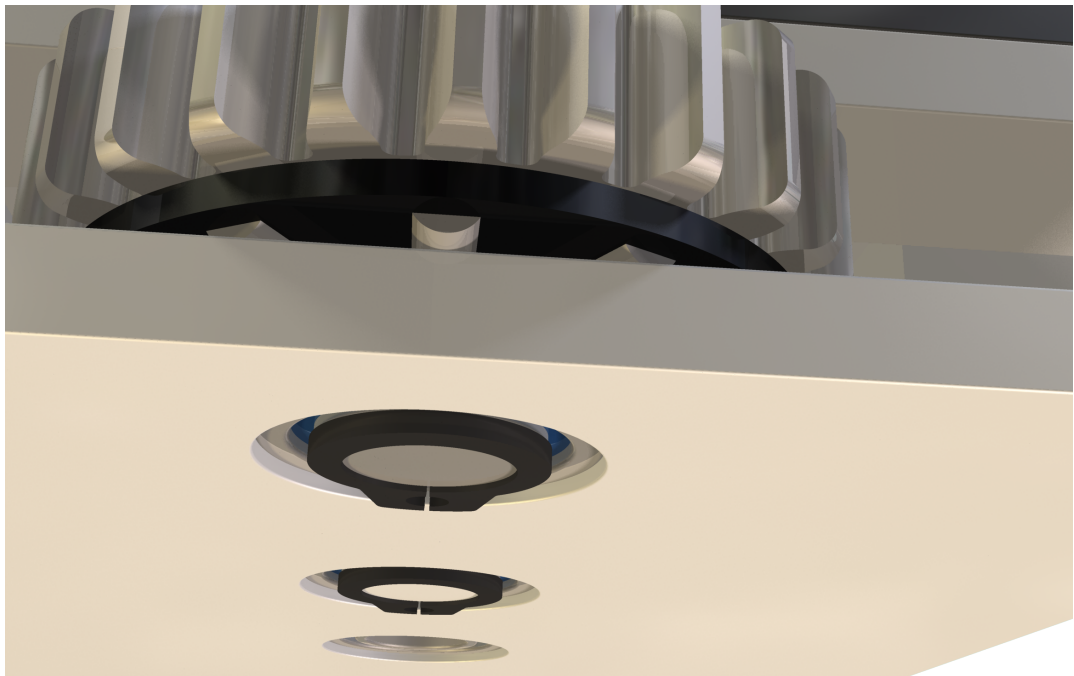


Figure A.17: A close up of the bearings, gears, and circlip

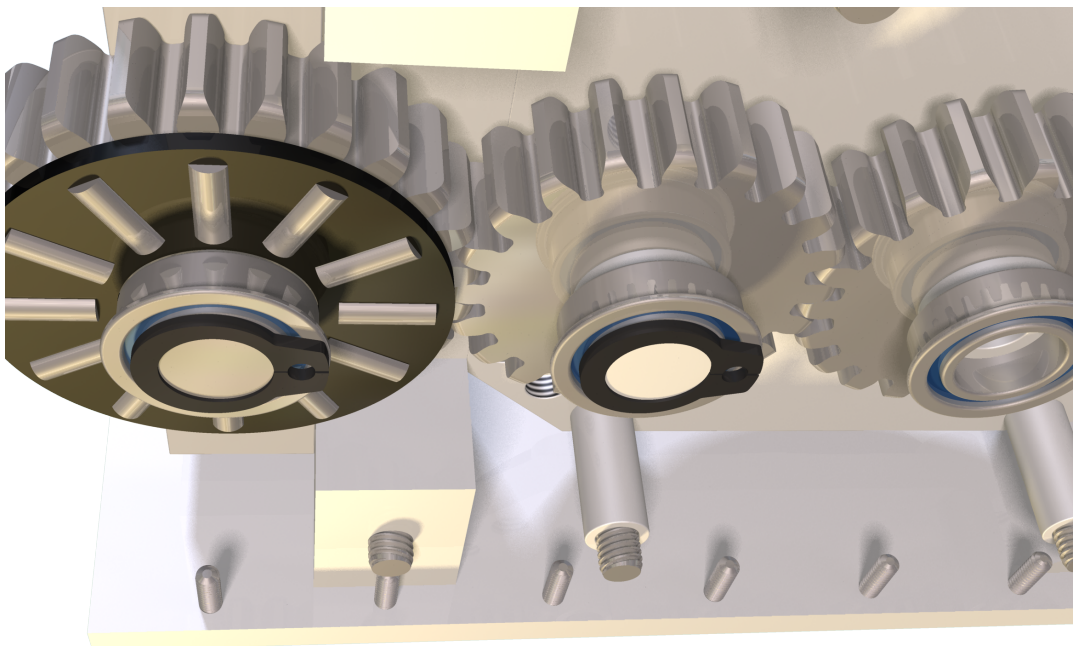
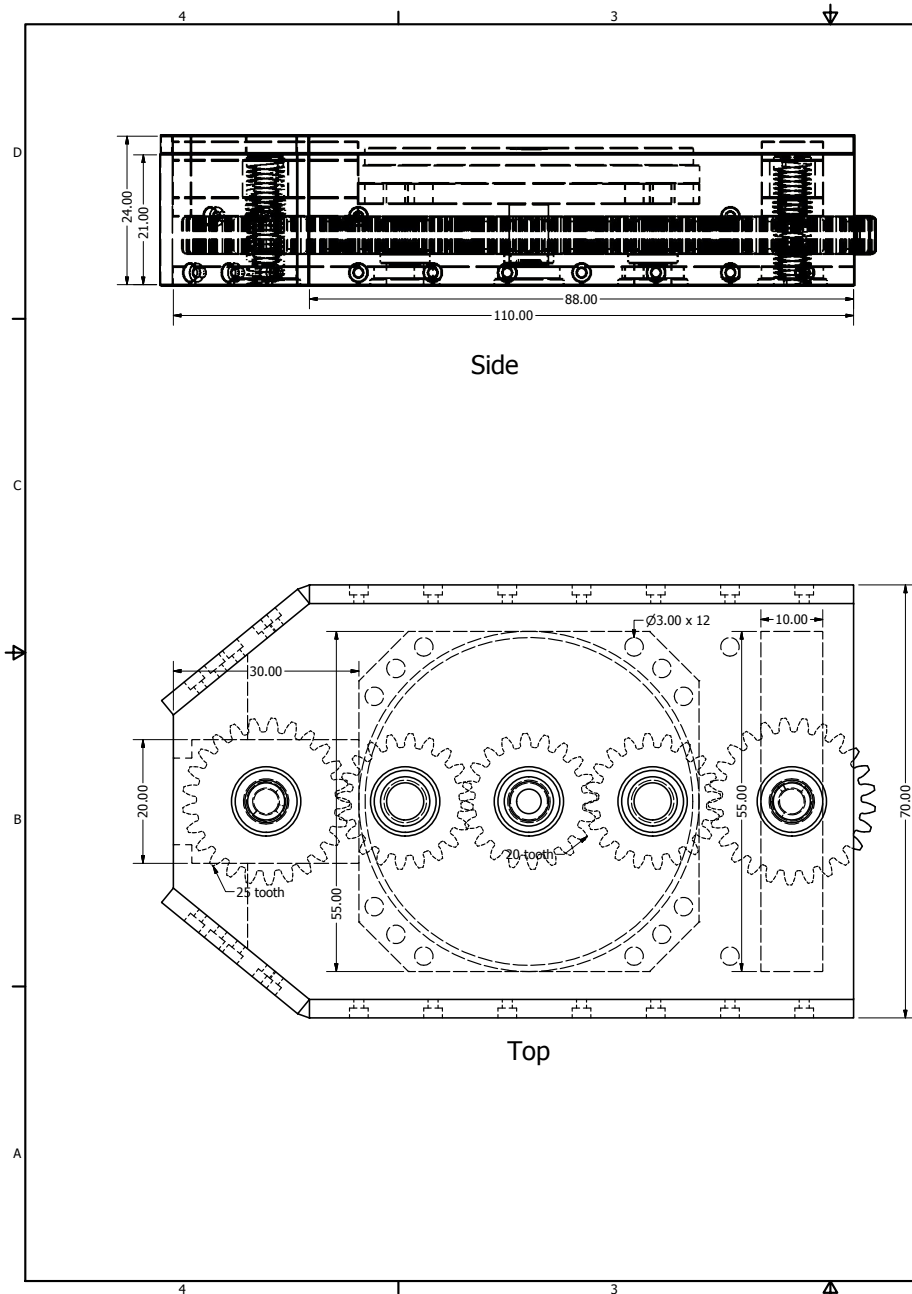


Figure A.18: A close up of the bearings, circlip, and gears, with the plate removed

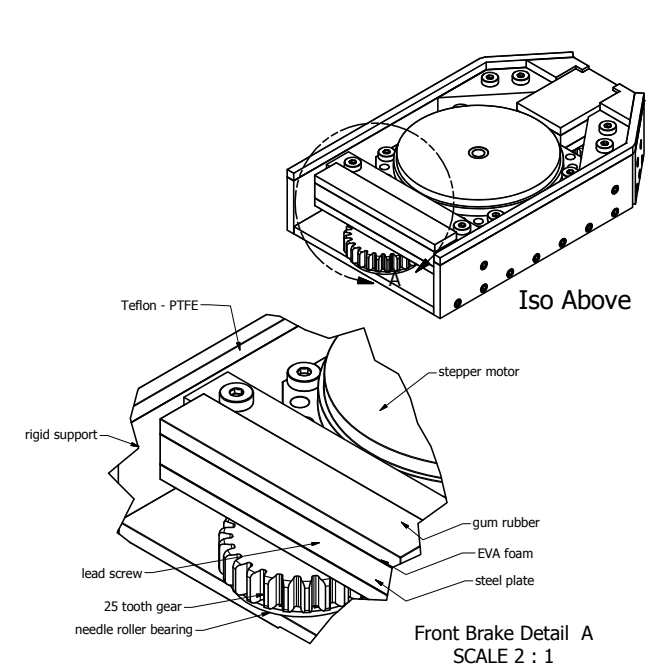
Appendix B

Machine Drawings

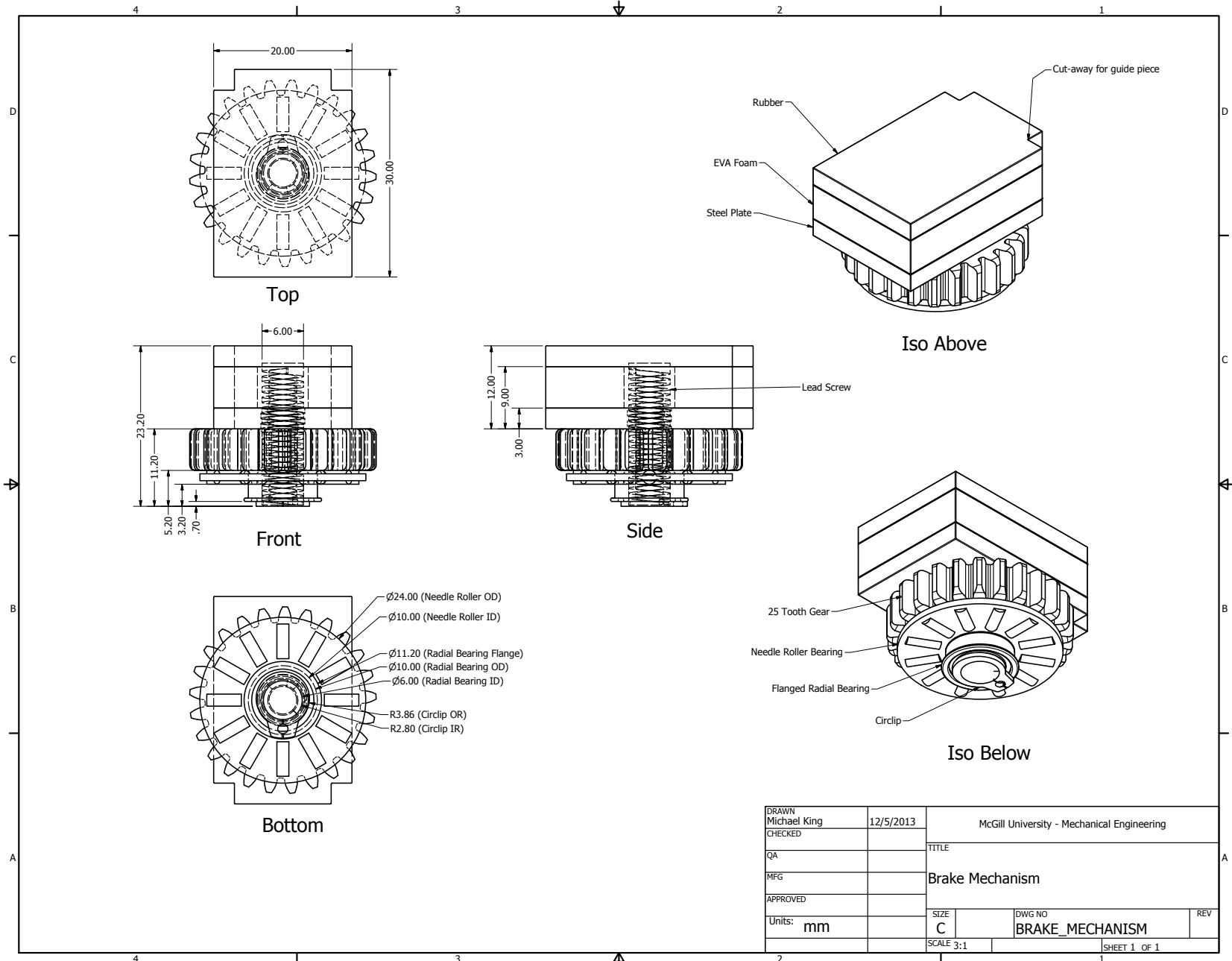
41



DRAWN	Michael King	12/4/2013	McGill University - Mechanical Engineering		
CHECKED			TITLE		
QA			Variable Friction Shoe Mechanism		
MFG					
APPROVED			SIZE	DWG NO	REV
UNITS:	mm	C	MASTER-ASSEMBLY		
			SCALE 2:1	SHEET 1 OF 1	



42



Appendix C

Product Specifications

Boundary Dimensions (mm)			Basic Load Ratings (N)		Limiting Speeds (min ⁻¹)	Bearing Numbers	Bearing Numbers of Matching Bearing Rings					NSKHPS
D _{c1} ,D _{p1}	D _c ,D _p	D _w	C _a	C _{0a}			Oil	s=1.0	s=1.5	s=2.0	s=2.5	
10	24	2	7750	23000	17000	FNTA-1024	FTRA-1024	FTRB-1024	FTRC-1024	-	-	
12	26	2	8350	26300	16000	FNTA-1226	FTRA-1226	FTRB-1226	FTRC-1226	-	-	
15	28	2	7950	25800	15000	FNTA-1528	FTRA-1528	FTRB-1528	FTRC-1528	FTRD-1528	FTRE-1528	
16	29	2	8200	27100	14000	FNTA-1629	FTRA-1629	FTRB-1629	FTRC-1629	FTRD-1629	FTRE-1629	
17	30	2	8400	28400	14000	FNTA-1730	FTRA-1730	FTRB-1730	FTRC-1730	FTRD-1730	FTRE-1730	
18	31	2	8600	29700	13000	FNTA-1831	FTRA-1831	FTRB-1831	FTRC-1831	FTRD-1831	FTRE-1831	
20	35	2	11900	47000	12000	FNTA-2035	FTRA-2035	FTRB-2035	FTRC-2035	FTRD-2035	FTRE-2035	
25	42	2	14800	66000	9500	FNTA-2542	FTRA-2542	FTRB-2542	FTRC-2542	FTRD-2542	FTRE-2542	
30	47	2	16500	79000	8500	FNTA-3047	FTRA-3047	FTRB-3047	FTRC-3047	FTRD-3047	FTRE-3047	
35	52	2	17300	88000	8000	FNTA-3552	FTRA-3552	FTRB-3552	FTRC-3552	FTRD-3552	FTRE-3552	
40	60	3	26900	122000	6700	FNTA-4060	FTRA-4060	FTRB-4060	FTRC-4060	FTRD-4060	FTRE-4060	
45	65	3	28700	137000	6300	FNTA-4565	FTRA-4565	FTRB-4565	FTRC-4565	FTRD-4565	FTRE-4565	
50	70	3	30500	152000	5600	FNTA-5070	FTRA-5070	FTRB-5070	FTRC-5070	FTRD-5070	FTRE-5070	
55	78	3	37000	201000	5300	FNTA-5578	FTRA-5578	FTRB-5578	FTRC-5578	FTRD-5578	FTRE-5578	
60	85	3	43000	252000	4800	FNTA-6085	FTRA-6085	FTRB-6085	FTRC-6085	FTRD-6085	FTRE-6085	
65	90	3	45500	274000	4500	FNTA-6590	FTRA-6590	FTRB-6590	FTRC-6590	FTRD-6590	FTRE-6590	
70	95	4	59000	320000	4300	FNTA-7095	FTRA-7095	FTRB-7095	FTRC-7095	FTRD-7095	FTRE-7095	
75	100	4	60000	335000	4000	FNTA-75100	FTRA-75100	FTRB-75100	FTRC-75100	FTRD-75100	FTRE-75100	
80	105	4	63000	365000	3800	FNTA-80105	FTRA-80105	FTRB-80105	FTRC-80105	FTRD-80105	FTRE-80105	
85	110	4	64500	380000	3600	FNTA-85110	FTRA-85110	FTRB-85110	FTRC-85110	FTRD-85110	FTRE-85110	
90	120	4	80000	515000	3400	FNTA-90120	FTRA-90120	FTRB-90120	FTRC-90120	FTRD-90120	FTRE-90120	
100	135	4	98500	695000	3000	FNTA-100135	FTRA-100135	FTRB-100135	FTRC-100135	FTRD-100135	FTRE-100135	

メートル系 フランジ付き単列深溝玉軸受

Single-row deep groove ball bearings with flanged outer ring (Metric series)

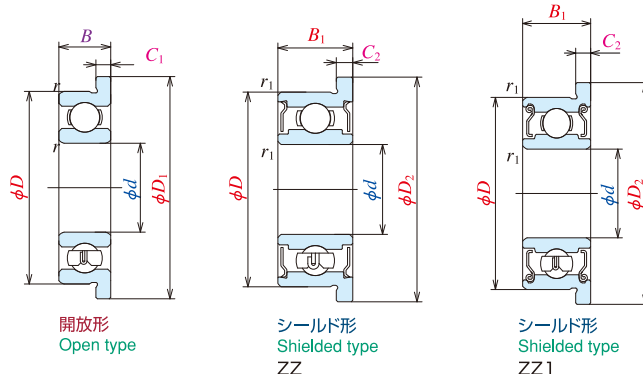
F600 形

F600, MF

MF 形

内径 5~9mm

Bore diameter 5~9mm



開放形 Open	呼び番号 Bearing numbers			主要寸法(mm) Boundary dimensions								基本定格荷重 Basic load ratings				
	シールド形 Shielded	シールド形 Sealed	シールド形 Sealed	d	D	D ₁	D ₂	B	B ₁	C ₁	C ₂	r _{最小 min}	r _{1 最小 min}	(N) C _r	{kgf} C _{or}	
MF85	—	—	—	5	8	9.2	—	2	—	0.6	—	0.10	—	310	120	31 12
—	MF85ZZ	—	—		8	—	9.2	—	2.5	—	0.6	—	0.10	278	131	28 13
MF95	MF95ZZ	—	—		9	10.2	10.2	2.5	3	0.6	0.6	0.15	0.15	430	168	44 17
MF105	MF105ZZ	—	—		10	11.2	11.6	3	4	0.6	0.8	0.15	0.15	430	168	44 17
F685	F685ZZ	—	—		11	12.5	12.5	3	5	0.8	1	0.15	0.15	715	281	73 29
F695	F695ZZ1	VV	DD		13	15	15	4	4	1	1	0.20	0.20	1080	430	110 44
F605	F605ZZ	—	DD		14	16	16	5	5	1	1	0.20	0.20	1330	505	135 52
F625	F625ZZ1	VV	DD		16	18	18	5	5	1	1	0.30	0.30	1730	670	177 68
F635	F635ZZ1	VV	DD		19	22	22	6	6	1.5	1.5	0.30	0.30	2340	885	238 90
MF106	MF106ZZ1	—	—	6	10	11.2	11.2	2.5	3	0.6	0.6	0.15	0.10	495	218	51 22
MF126	MF126ZZ	—	DD		12	13.2	13.6	3	4	0.6	0.8	0.20	0.15	715	292	73 30
F686A	F686AZZ1	VV	DD		13	15	15	3.5	5	1	1.1	0.15	0.15	1080	440	110 45
F696	F696ZZ1	VV	DD		15	17	17	5	5	1.2	1.2	0.20	0.20	1730	670	177 68
F606	F606ZZ	VV	DD		17	19	19	6	6	1.2	1.2	0.30	0.30	2260	835	231 85
F626	F626ZZ1	VV	DD		19	22	22	6	6	1.5	1.5	0.30	0.30	2340	885	238 90
F636	F636ZZ	VV	DD		22	25	25	7	7	1.5	1.5	0.30	0.30	3300	1370	335 140
MF117	MF117ZZ	—	—	7	11	12.2	12.2	2.5	3	0.6	0.6	0.15	0.10	455	201	47 21
MF137	MF137ZZ	—	—		13	14.2	14.6	3	4	0.6	0.8	0.20	0.15	540	276	55 28
F687	F687ZZ1	VV	DD		14	16	16	3.5	5	1	1.1	0.15	0.15	1170	510	120 52
F697	F697ZZ1	VV	DD		17	19	19	5	5	1.2	1.2	0.30	0.30	1610	710	164 73
F607	F607ZZ1	VV	DD		19	22	22	6	6	1.5	1.5	0.30	0.30	2340	885	238 90
F627	F627ZZ	VV	DD		22	25	25	7	7	1.5	1.5	0.30	0.30	3300	1370	335 140
MF128	MF128ZZ1	VV	DD	8	12	13.2	13.6	2.5	3.5	0.6	0.8	0.15	0.10	545	274	56 28
MF148	MF148ZZ	VV	DD		14	15.6	15.6	3.5	4	0.8	0.8	0.20	0.15	820	385	83 39
F688A	F688AZZ1	VV	DD		16	18	18	4	5	1	1.1	0.20	0.20	1610	710	164 73
F698	F698ZZ1	VV	DD		19	22	22	6	6	1.5	1.5	0.30	0.30	2240	910	228 93
F689	F689ZZ	VV	DD	9	17	19	19	4	5	1	1.1	0.20	0.20	1330	665	136 68

注 (*1) 外径、内径の実寸法を示します。

Notes Actual dimensions of bore and outside diameter only.

(2) ステンレス品の基本動定格荷重は0.85掛けが目安となります。

The rough standard of basic dynamic load rating for stainless products would be 15% less than the value appeared in the list.

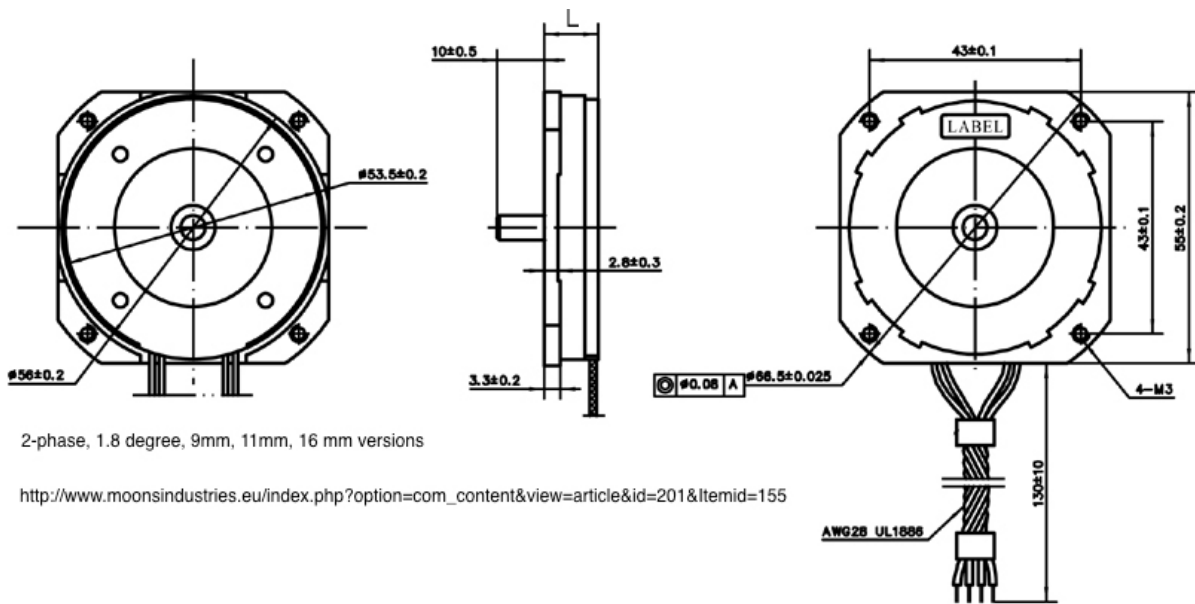


Figure C.3: Moon's Industries 23HY9401 Pancake Super Flat 2-Phase Stepper Motor

Appendix D

Photos

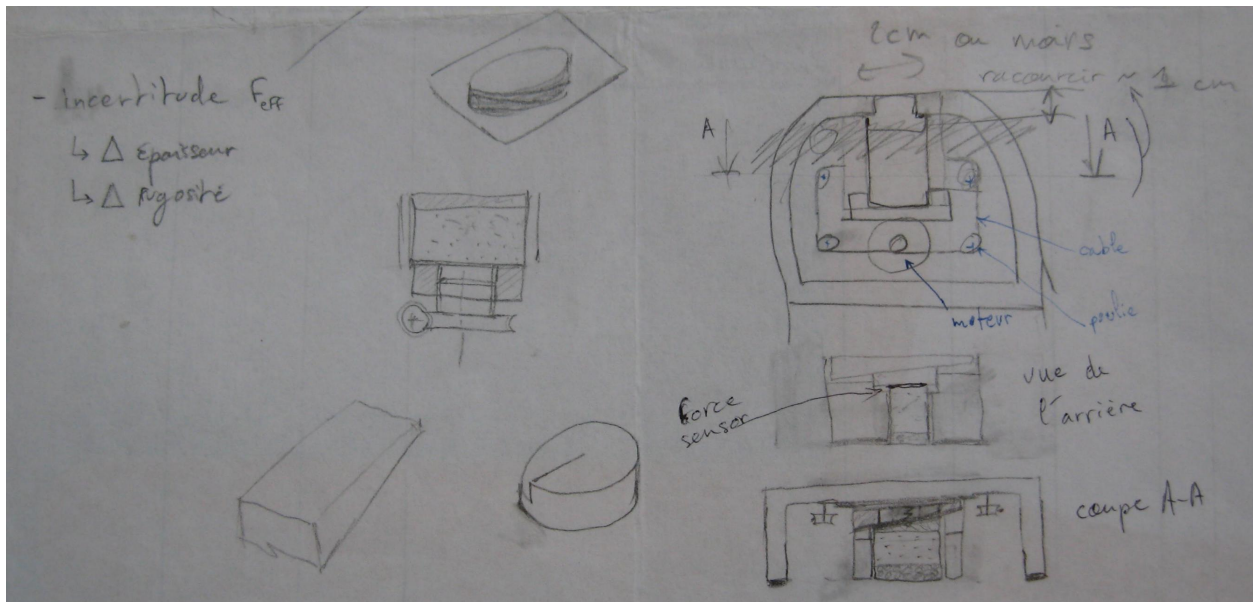


Figure D.1: Very preliminary sketch by G. Millet

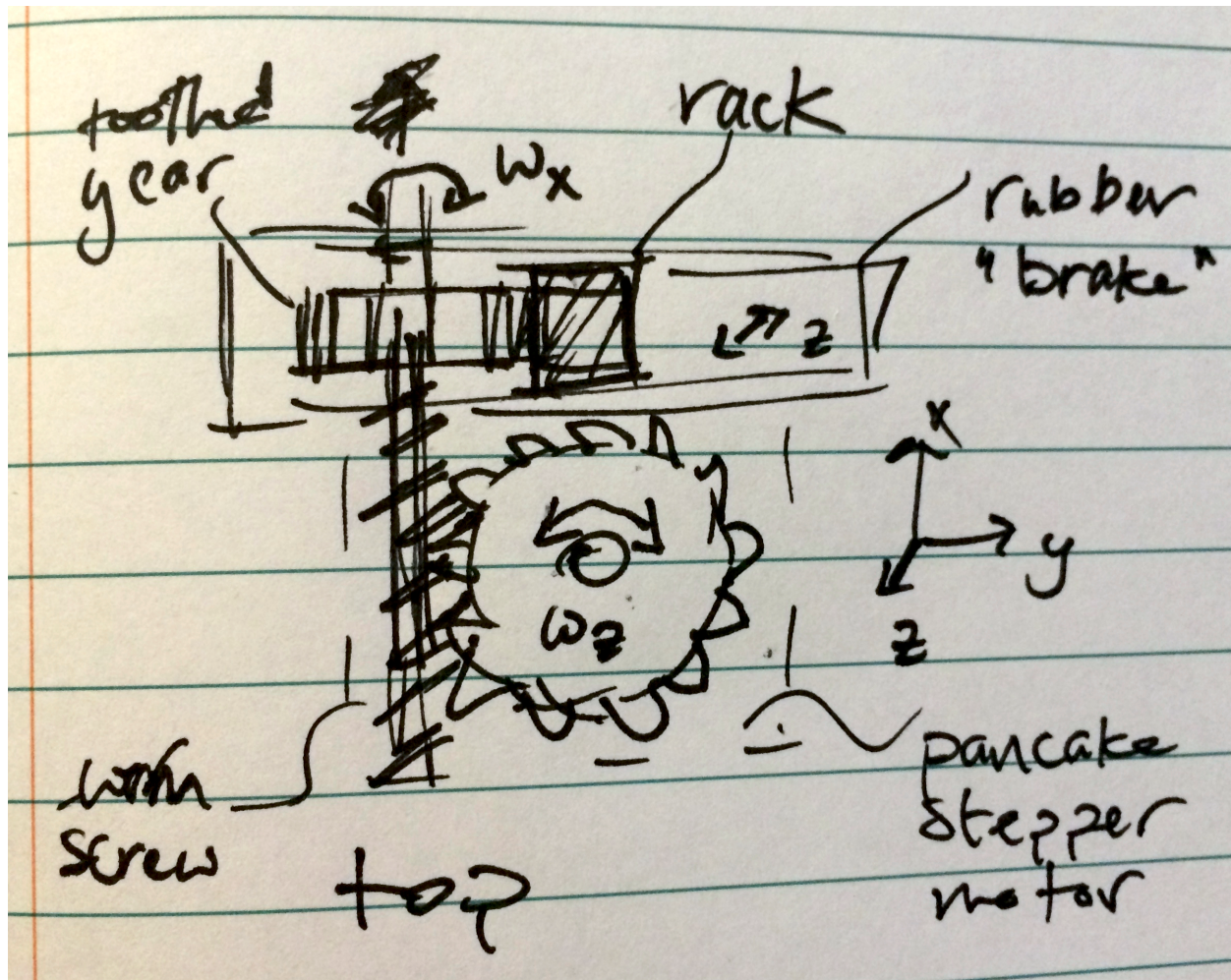
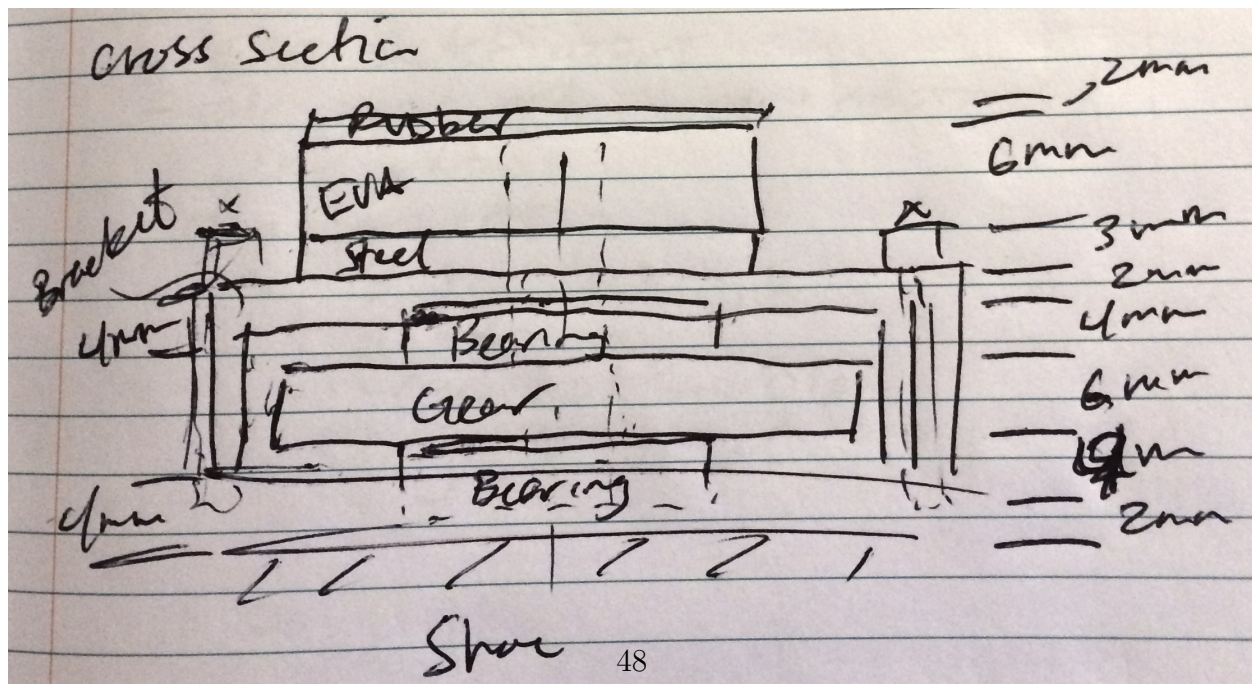


Figure D.2: Preliminary sketch of worm gear idea



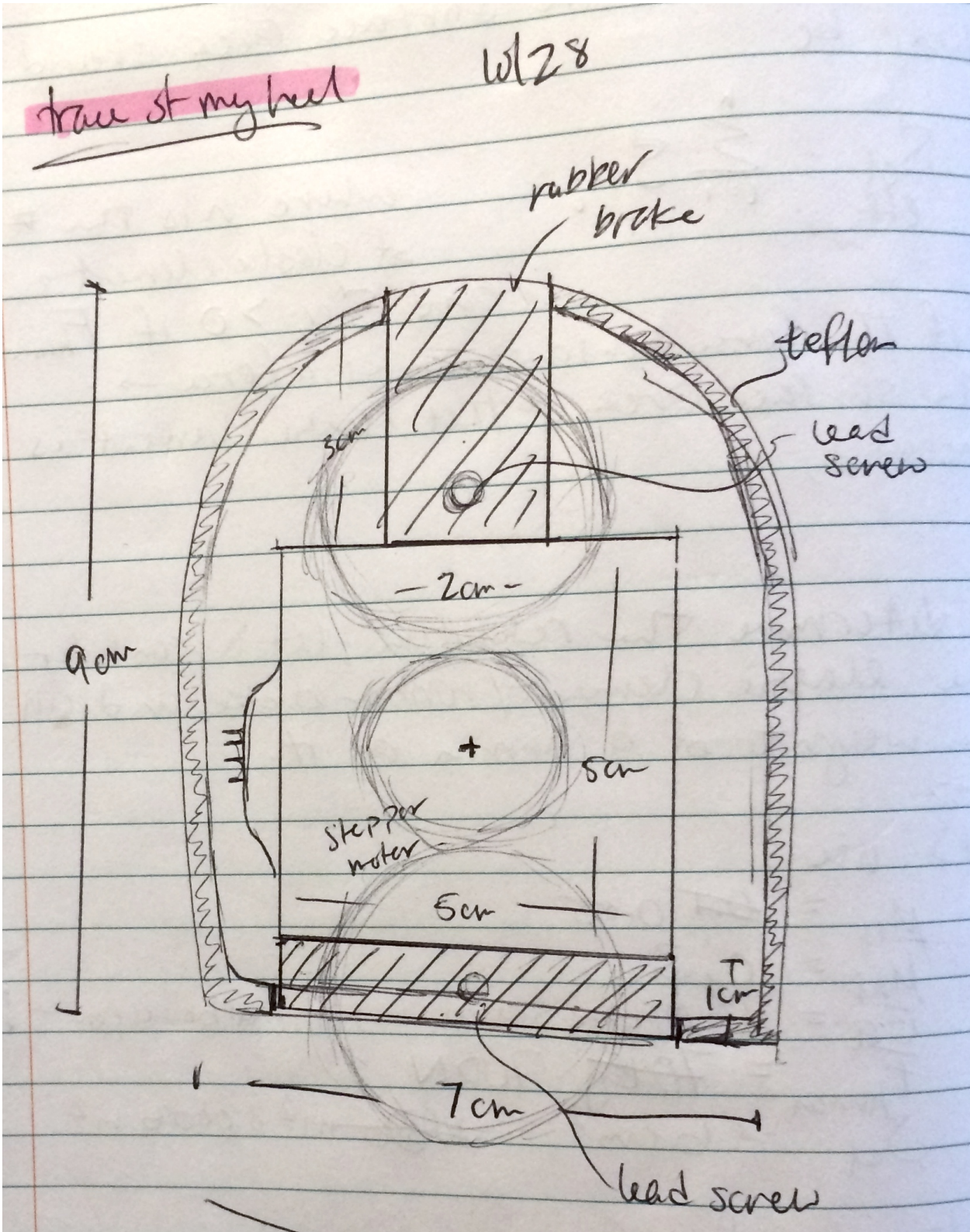


Figure D.3: Preliminary sketch of lead screw idea